

ACOUSTIC TRACKING OF SHIP WAKES

A THESIS SUBMITTED TO
THE GRADUATE SCHOOL OF NATURAL AND APPLIED SCIENCES
OF
MIDDLE EAST TECHNICAL UNIVERSITY

BY

ÇAĞLA ÖNÜR

IN PARTIAL FULFILLMENT OF THE REQUIREMENTS
FOR
THE DEGREE OF DOCTOR OF PHILOSOPHY
IN
ELECTRICAL AND ELECTRONICS ENGINEERING

JANUARY 2013

Approval of the thesis:

ACOUSTIC TRACKING OF SHIP WAKES

submitted by **ÇAĞLA ÖNÜR** in partial fulfillment of the requirements for the degree of **Doctor of Philosophy in Electrical and Electronics Engineering Department, Middle East Technical University** by,

Prof. Dr. Canan Özgen
Dean, Graduate School of **Natural and Applied Sciences** _____

Prof. Dr. İsmet Erkmen
Head of Department, **Electrical and Electronics Engineering** _____

Prof. Dr. Kemal Leblebicioğlu
Supervisor, **Electrical and Electronics Engineering Dept., METU** _____

Examining Committee Members:

Prof. Dr. Yasemin Yardımcı Çetin
Informatics Institute, METU _____

Prof. Dr. Kemal Leblebicioğlu
Electrical and Electronics Engineering Dept., METU _____

Prof. Dr. Billur Barshan
Electrical and Electronics Engineering Dept., Bilkent University _____

Assoc. Prof. Dr. Afşar Saranlı
Electrical and Electronics Engineering Dept., METU _____

Assoc. Prof. Dr. İlkey Ulusoy
Electrical and Electronics Engineering Dept., METU _____

Date: 30.01.2013

I hereby declare that all information in this document has been obtained and presented in accordance with academic rules and ethical conduct. I also declare that, as required by these rules and conduct, I have fully cited and referenced all material and results that are not original to this work.

Name, Last name: Çaęla Önür

Signature :

ABSTRACT

ACOUSTIC TRACKING OF SHIP WAKES

Önür, Çağla

Ph.D., Department of Electrical and Electronics Engineering
Supervisor: Prof. Dr. Kemal Leblebicioğlu

January 2013, 78 pages

Theories about ship wake structure, bubble dynamics, acoustic propagation through bubble clouds, backscattering and target strength of bubble clouds have been investigated and related Matlab simulations have been carried on. Research has been carried on algorithms for ship wake acoustic detection and tracking. Particle filter method has been simulated with Matlab for target tracking using wake echo measurements. Simulation results are promising.

Keywords: Acoustic, Bubble, Wake, Tracking.

ÖZ

GEMİLERİN DÜMEN SUYUNUN AKUSTİK TAKİBİ

Önür, Çağla

Doktora, Elektrik ve Elektronik Mühendisliği Bölümü
Tez Yöneticisi: Prof. Dr. Kemal Leblebicioğlu

Ocak 2013, 78 sayfa

Gemi dümen suyu yapısı, kabarcık dinamiği, kabarcık bulutları arasında akustik yayılım, kabarcık bulutlarının geri saçılımı ve hedef kuvveti ile ilgili teoriler üzerinde çalışılmış ve ilgili Matlab benzetimleri yürütülmüştür. Gemilerin dümen suyunun akustik tespiti ve takibi için algoritmalar üzerine araştırma yürütülmüştür. Dümen suyu eko ölçümlerini kullanarak hedef takibi yapabilmek için parçacık filtresi metodunun Matlab'da benzetimi gerçekleştirilmiştir. Benzetim sonuçları umut vericidir.

Anahtar Kelimeler: Akustik, Kabarcık, Dümen Suyu, Takip.

To My Parents

ACKNOWLEDGMENTS

The author would like to thank her supervisor Prof. Dr. Kemal Leblebiciođlu for his guidance and encouragement throughout the research.

The author would like to thank the company she works for, STM Savunma Teknolojileri Mühendislik ve Ticaret A.Ş., for their support.

The author would like to thank her parents and sister for their affection and support throughout her life.

TABLE OF CONTENTS

ABSTRACT.....	v
ÖZ.....	vi
ACKNOWLEDGMENTS.....	viii
TABLE OF CONTENTS.....	ix
CHAPTER	
1. INTRODUCTION.....	1
1.1 Literature.....	1
1.2 Contributions.....	3
1.3 Thesis Plan.....	4
2. BUBBLE THEORY.....	5
2.1 Bubble Dynamics.....	5
2.2 Acoustic Propagation through Bubble Clouds.....	9
2.3 Backscattering and Target Strength of Bubble Clouds.....	20
3. SHIP WAKE ECHO.....	25
3.1 Ship Wake Structure.....	25
3.2 Ship Wake Echo.....	34
4. ACOUSTIC DETECTION AND TRACKING OF SHIP WAKES.....	37
4.1 Introduction.....	37
4.2 Wake Features for Detection and Tracking.....	37
4.3 Tracking with Particle Filter.....	42
5. CONCLUSIONS.....	59
REFERENCES.....	61
VITA.....	78

LIST OF TABLES

TABLES

Table 3.1 Void fraction and bubble density values.....	29
Table 3.2 Bubble size distribution.....	34
Table 4.1 Probability $p(M r)$ forming the perception model.....	45

LIST OF FIGURES

FIGURES

Figure 2.1 Average attenuation coefficient versus number of bubbles.....	14
Figure 2.2 Average sound speed versus number of bubbles.....	14
Figure 2.3 Average attenuation coefficient versus source frequency.....	15
Figure 2.4 Average sound speed versus source frequency.....	15
Figure 2.5 Average attenuation coefficient for a Gaussian bubble size distribution.....	16
Figure 2.6 Average sound speed for a Gaussian bubble size distribution.....	16
Figure 3.1 Representation of wake axes.....	26
Figure 3.2 Bubble density profile of the simulated wake.....	28
Figure 3.3 Receive level profile measurement scenario.....	35
Figure 3.4 Receive level profile when insonifying the wake from the side.....	36
Figure 3.5 Receive level profile when insonifying the wake from the side with background noise added.....	36
Figure 4.1 Measurement configuration for receive level summation.....	38
Figure 4.2 Receive level summation along the wake range at 1 m depth.....	39
Figure 4.3 Receive level at 600 m wake range and 1 m depth.....	39
Figure 4.4 Receive level profile with 1 kHz source.....	40
Figure 4.5 Receive level profile with 10 kHz source.....	40
Figure 4.6 Receive level profile with 30 kHz source.....	41
Figure 4.7 Receive level profile with 200 kHz source.....	41
Figure 4.8 Tracking algorithm.....	47
Figure 4.9 Real and estimated coordinates of the target.....	47
Figure 4.10 RMSE value for the target ship location estimates.....	48
Figure 4.11 Real and estimated coordinates of the target.....	49
Figure 4.12 Real and estimated x-coordinate values of the target.....	49
Figure 4.13 Real and estimated y-coordinate values of the target.....	50

Figure 4.14 Coordinates of the target ship and the underwater vehicle.....	52
Figure 4.15 RMSE value for the target ship x-coordinate estimates.....	53
Figure 4.16 RMSE value for the target ship y-coordinate estimates.....	53
Figure 4.17 RMSE value for the target ship location estimates.....	54
Figure 4.18 Coordinates of the target ship and the underwater vehicle.....	55
Figure 4.19 RMSE value for the target ship x-coordinate estimates.....	56
Figure 4.20 RMSE value for the target ship y-coordinate estimates.....	56
Figure 4.21 RMSE value for the target ship location estimates.....	57

CHAPTER 1

INTRODUCTION

1.1 Literature

In the scope of underwater warfare, strong signature of ship wakes is attractive for its exploitation in ship detection, tracking and classification. It is known that nations are working on the development of wake-homing torpedoes and counter-measures against wake-homing torpedoes.

Ship wake signatures are generally more distinct than the signature of the ship. Also information about the ship's heading and speed can be obtained from the wake pattern. The most effective underwater sensor for detection is sonar. Detection and tracking of surface ships using radar may be difficult due to the low signal to clutter ratio and wake detection using sonar may be preferable [66].

The strong signature of ship wakes is due to bubbles found inside them. Ships generate bubbles by propeller cavitation, by breaking of ship generated waves, and by air entrapment in the turbulent boundary layer under the ship hull [6]. As bubbles breakup, turbulent diffusion causes bubbles to mix and fragment. Afterwards, turbulence decays and the bubbles of different sizes begin to rise at different rates towards the surface due to their buoyancy. The main physical processes affecting the bubbles in this phase are advection by local currents, turbulent diffusion, buoyant degassing, and dissolution [1, 29].

Ship propeller and hull design, ship speed and maneuver affect the bubble distribution and hence wake signature [6, 10, 15]. In various experiments, it has been observed that ship wakes could last for about 15 minutes [1, 15].

As it will be detailed in the next chapter, bubbles are nonlinear oscillators. They act as acoustic sources giving out characteristic acoustic emissions depending on their entrainment procedure. Also they affect acoustic propagation such that acoustic waves through the bubble cloud have frequency dependent average sound speed and attenuation. Backscattering of the acoustic waves is observed due to the scattering cross sections of the bubbles. These properties of bubbles create the acoustic signature of ship wakes [2, 8].

Since 1940's, various research have been made trying to understand the effects of bubble clouds and the inverse problem of characterizing the structure of bubble clouds [1-26, 29-31].

Various acoustic methods are used for probing underwater bubble clouds to estimate parameters like average sound speed, average attenuation, target strength, bubble size distribution and void fraction. Mostly used acoustic methods for probing bubble clouds are pulsed and continuous wave forward propagation measurements using separate projector and hydrophones, backscatter measurements using multi-beam sonars, and measurements using acoustic resonators. While each method has different advantages making it suitable for bubble clouds with specific structures, best approach seems to be using a combination of these methods [1, 3, 4].

Generally, for both forward and inverse problems, various simplifying assumptions are made such as bubbles undergo linear, steady-state monochromatic oscillations in the free field, without interacting. In reality, these assumptions fail more or less especially in specific cases.

Most of the developed theories are effective medium theories which treat two-phase bubbly mixtures as a single, homogenized medium. Hence, it is assumed that the locations of the bubbles are independent from each other. In order to accurately describe the acoustic propagation in clustered bubble clouds with void fractions sufficiently high to make interactions between bubbles considerable, modification of these theories by including correlation functions for the relationship between the positions of the bubbles is necessary [1, 21].

Effective medium theories developed for the propagation of sound through bubble clouds use different approaches like multiple scattering approach, continuum approximation approach, and diagram approach. These theories treat the propagation of acoustic waves through bubble clouds in a statistical sense which is preferable because of the variability inherent in bubble clouds [1, 30].

High driving pressures make the linear bubble dynamics assumption invalid. A case which necessitates the use of high driving acoustic pressure amplitudes might be probing of a medium with high void fractions causing high attenuation. High acoustic pressure amplitudes may be desirable also in low void fractions, because they offer opportunities to gain information about the bubble cloud or to enhance sonar operation by the exploitation of nonlinear effects [13, 18-20].

Adjusting various parameters of the insonifying signal, exploitation of nonlinear effects in bubble clouds is possible. Actually it seems that marine mammals use echolocation signals exploiting these nonlinear effects [13, 18, 24].

The resonant bubble approximation depends on the assumption that only the bubbles at resonance with the insonifying field contribute significantly to attenuation. It has been shown by various studies that including the effect of off-resonance contributions improves the results of related estimations [9, 31].

In literature it is possible to find various experimental and theoretical work related to modeling the ship wake structure [6, 7, 10, 15, 16, 17, 26, 29, 68, 90, 100, 102, 103, 117, 125]. On the other hand, a complete model of the ship wake structure that includes the initial bubble distribution and the evolution of the bubble distribution in relation with the ship and ambient parameters does not exist in the open literature.

In [102], a ship wake model is formed for acoustic propagation studies. The mean bubble density profile of the ship wake is constructed from the data found in the literature. A separate stochastic function is used to form the random structure of the bubble density.

More complex wake models have also been constructed in the literature. In a recent work [103], it is stated that the wake of a ship is governed by the water current pattern in the wake. Bubbles are distributed in the water by the wake currents. Besides the acoustic signature created by the bubbles, the currents in the wake can also create an acoustic signature.

In [66], a detection and tracking algorithm is described to detect and track a ship. The strong noise created by propeller cavitation is used to estimate the bearing of the starting point of the wake. Then a linear feature corresponding to the wake is determined using a high frequency active sonar. This increases the confidence of target detection and also provides initial estimates of target position and velocity. Kalman filter is used for tracking the starting point of the wake, hence the target ship.

In literature [18], exploiting the nonlinear dynamics of the bubbles stands out as a promising method for detecting ship wakes. The insonifying signal could be adjusted such that while linear scatterers give little or no response, response from ship wake bubbles is high enough for detection.

There are also papers [17] dealing with modelling the echo signals of ship wakes insonified by an active sonar. Matched filter and energy detector are among the detectors used on the echo time series. The effect of parameters such as distance to the ship, the aspect angle, and the source frequency is investigated using the echo models developed.

1.2 Contributions

In this thesis, research is carried on ship wake acoustic detection and tracking. A simulation environment is developed in Matlab and results of related numerical experiments are given.

The wake model described in [102] is taken as the basis for the wake profiles used in this thesis. Since the mean bubble density profile of the wake model in [102] depends on data found in the literature, it is supposed that the wake model will give realistic and sufficient results for the studies related to this thesis.

The wake model described in [102] is simulated with some modifications. Mainly the bubble size distribution of the wake model is changed, taking into account that small sized bubbles last for a longer time than bigger sized bubbles.

Receive level profiles when insonifying ship wake are obtained using this wake model. Some features of the ship wake echo level pattern that could be exploited for detection and tracking are outlined.

Particle filter method is implemented for target tracking based on wake echo measurements. Particle filter method is used instead of Kalman filter method, since wake echo measurement is a nonlinear function of target position. Compared with the method in [66], it is not necessary for the target, namely the start point of the wake, to be inside the search range.

Two articles have been prepared from this thesis for submission [223, 224]:

- 1) Ç. Önür, K. Leblebicioğlu. "Ship Wake Acoustic Tracking Using Particle Filter". IEEE Journal of Oceanic Engineering, 2013.
- 2) Ç. Önür, K. Leblebicioğlu. "Wake Tracking with Particle Filter". 21. IEEE Sinyal İşleme ve İletişim Uygulamaları Kurultayı, 2013.

1.3 Thesis Plan

In Chapter 2, the theoretical information found in the literature about bubble dynamics, acoustic propagation through bubble clouds, and backscattering and target strength of bubble clouds is given. In Chapter 3, ship wake structure models found in the literature and the model used are explained. Also, examples for wake echo level profile obtained using the wake model are given. In Chapter 4, the algorithms for ship wake acoustic detection and tracking are explained. In the References chapter, there is an extensive list [1-224] of literature about bubble acoustic behavior, ship wake measurements, and target tracking.

CHAPTER 2

BUBBLE THEORY

2.1 Bubble Dynamics

For a static gas bubble in a liquid, the internal pressure P_{int} of the bubble which is formed by the pressure of the gas P_{gas} and the pressure of the liquid vapour P_{vap} inside the bubble is equal to the sum of the liquid pressure P_{liq} at the bubble wall and the pressure resulting from the surface tension P_{tens} that tries to keep the bubble intact. In equilibrium, the liquid pressure P_{liq} at the bubble wall is equal to the pressure in the liquid P_{∞} far away from the bubble [2].

An excess pressure inside the bubble that makes the pressure of the gas within the bubble greater than the dissolved gas in the liquid just outside the bubble is formed to balance the surface tension pressure. Hence, the bubble tends to dissolve. This causes the concentration of the dissolved gas in the liquid at the bubble wall to exceed the concentration far away from the bubble. As the bubble dissolves because of this concentration difference, the size of it reduces making the surface tension pressure increase. Hence, the general tendency of the bubble is to dissolve [2].

Bubbles are actually nonlinear oscillators. For simplicity, they are modeled as linear oscillators. The equation of motion for a bubble as a linear oscillator driven by a force can be written as

$$m \frac{d^2 \varepsilon}{dt^2} + b \frac{d\varepsilon}{dt} + s\varepsilon = F \quad (2.1)$$

where m is the mass, b is the damping coefficient, s is the stiffness, F is the force applied on the bubble, and ε is the associated radial displacement of the bubble wall [1, 2].

Mass in Eq. (2.1) is actually equal to the mass of the entrained fluid which is three times the mass of the fluid displaced by the bubble. So m is given by

$$m = \rho_o 4\pi a^3, \quad (2.2)$$

where ρ_o is the fluid density and a is the bubble radius [1].

If the gas inside the bubble is assumed to behave as an ideal gas, the relation between pressure inside the bubble and the bubble volume can be written as

$$P_{\text{int}} V^{\gamma(d+j\epsilon)} = C, \quad (2.3)$$

where γ is the ratio of specific heats for the gas inside the bubble, d and e account for the changes in γ , and C is a constant [1].

The damping coefficient and the stiffness for the bubble in Eq. (2.1) are given by [1]

$$b = \frac{12\pi a \gamma e P_{\text{int}}}{w} , \quad (2.4)$$

$$s = 12\pi a \gamma d P_{\text{int}} , \quad (2.5)$$

where $w = 2\pi f$ is the angular frequency of oscillation.

Since the bubble is modeled as a linear harmonic oscillator, its angular resonance frequency is the square root of the ratio of the bubble stiffness to the mass of the entrained fluid which can be written as [1]

$$w_o = 2\pi f_o = \frac{1}{a} \sqrt{\frac{3\gamma d P_{\text{int}}}{\rho_o}} . \quad (2.6)$$

The damping constant for the linear oscillator defined by Eq. (2.1) is given by

$$\delta = b / w m \quad (2.7)$$

and for the bubble, it is the summation of three components: the damping constant δ_r due to radiation, the damping constant δ_t due to thermal conductivity, and the damping constant δ_v due to shear viscosity. Hence it can be expressed as [2, 3]

$$\delta = \delta_r + \delta_t + \delta_v . \quad (2.8)$$

Different formulations exist in the literature for the damping constants. In [2], under some assumptions, they are formulated as:

$$\delta_r = \frac{w_o \times a}{c} \quad (2.9)$$

$$\delta_t = 4.41 \times 10^{-4} \sqrt{f_o} \quad (2.10)$$

$$\delta_v = \frac{410}{w_o} . \quad (2.11)$$

The energy subtracted by the bubble from the energy of an incident acoustic wave is represented by the extinction cross-section which is the summation of the scattering and absorption cross-sections of the bubble. The absorption cross-section is the summation of the thermal dissipation and viscous dissipation cross-sections. The ratio of the energy losses due to radiation, thermal conductivity, and shear viscosity, hence the ratio of the related cross-sections, are in the ratio of the related damping constants [2].

If an oscillating force with frequency f is applied to the bubble, according to the linear equation in Eq. (2.1), the bubble wall will oscillate with the same frequency. Hence, if $F = Me^{j\omega t}$ is the applied force, the radial bubble wall displacement is given by $\varepsilon = De^{j\omega t}$. The radially oscillating bubble creates a spherically symmetric radiation field. The pressure for this radiation field can be written as

$$P_{sct} = A \frac{e^{j(\omega t - kr)}}{r}, \quad (2.12)$$

where A is the amplitude of the scattered pressure wave at one meter distance from the bubble, r is the distance from the bubble, and $k = 2\pi/\lambda$ is the wavenumber where λ is the wavelength [1].

Using $F = Me^{j\omega t}$ and $\varepsilon = De^{j\omega t}$ in Eq. (2.1), the amplitude D of the radial bubble wall displacement is found as

$$D = \frac{1}{w^2 m} \frac{P_{inc} 4\pi a^2}{\left[\frac{w_0^2}{w^2} - 1 \right] + j\delta}, \quad (2.13)$$

where P_{inc} is the amplitude of the incident pressure [1].

The particle velocity for the spherical radiation field of the bubble can be written as

$$u = jw\varepsilon \quad (2.14)$$

in terms of the bubble wall displacement.

Using the relation

$$\frac{\partial P_{sct}}{\partial r} = -\rho \frac{\partial u}{\partial t} \quad (2.15)$$

and Eq. (2.7), the scattered spherical pressure field in relation to the particle velocity is found as [1, 32]

$$P_{sct} = \frac{\rho_0 c}{\left(1 - \frac{j}{kr}\right)} u. \quad (2.16)$$

Using Eq. (2.7), Eq. (2.8), Eq. (2.12), Eq. (2.14), and assuming that $ka \ll 1$, the amplitude A of the scattered pressure wave one meter away from the bubble is

found to be [1]

$$A = \frac{P_{inc} a e^{jka}}{\left(\frac{w_o^2}{w^2} - 1\right) + j\delta} . \quad (2.17)$$

The scattering coefficient s of the bubble is defined as the ratio of the amplitude of the scattered pressure wave to the amplitude of the incident pressure wave. Hence, the scattering coefficient is given by [1]

$$s = \frac{A}{P_{inc}} = \frac{a e^{jka}}{\left(\frac{w_o^2}{w^2} - 1\right) + j\delta} . \quad (2.18)$$

The scattering cross section of the bubble is defined as the ratio of the total scattered power to the incident intensity. Therefore, it is given by [1]

$$\sigma_s = 4\pi \frac{|A|^2}{|P_{inc}|^2} = \frac{4\pi a^2}{\left(\frac{w_o^2}{w^2} - 1\right)^2 + \delta^2} . \quad (2.19)$$

Since the damping constant due to radiation is given by $\delta_r = ka$, the absorption cross-section and the extinction cross-section can be written as [2, 19]

$$\sigma_a = \frac{4\pi a^2 \left(\frac{\delta}{ka} - 1\right)}{\left(\frac{w_o^2}{w^2} - 1\right)^2 + \delta^2} \quad (2.20)$$

and

$$\sigma_e = \frac{4\pi a^2 \left(\frac{\delta}{ka}\right)}{\left(\frac{w_o^2}{w^2} - 1\right)^2 + \delta^2} . \quad (2.21)$$

Although the linear model given above is used for simplifying the things, as mentioned before, bubbles are nonlinear oscillators. One of the cases where the necessity of using a nonlinear model arises is the case of high driving pressures. Since the bubble has a finite radius, increasing the amplitude of the driving pressure cannot increase the amplitude of the scattered pressure in proportion [19].

Examining the physics of the oscillation process, various formulations giving the relationship between the bubble response and the driving pressure have been

derived. One of those formulations is the modified Herring-Keller equation given by

$$a\ddot{a}\left(1-\frac{\dot{a}}{c}\right)+\frac{3}{2}\dot{a}^2\left(1-\frac{1}{3}\frac{\dot{a}}{c}\right)=\left(1+\frac{\dot{a}}{c}\right)\frac{1}{\rho}\left(p_{liq}-p_o-p_{inc}\left(t+\frac{a}{c}\right)\right)+\frac{a}{\rho c}\frac{dp_{liq}(t)}{dt}, \quad (2.22)$$

where a is the bubble radius, \dot{a} is the instantaneous bubble wall velocity, \ddot{a} is the instantaneous bubble wall acceleration, p_o is the hydrostatic pressure in the liquid, p_{liq} is the liquid pressure at the bubble wall, and p_{inc} is the driving pressure [2, 24].

The liquid pressure at the bubble wall is given as

$$p_{liq}=\left(p_o+\frac{2\sigma}{a}\right)\left(\frac{a}{a_e}\right)^{3\kappa}-\frac{2\sigma}{a}-\frac{4\eta_l\dot{a}}{a}, \quad (2.23)$$

where η_l is the shear viscosity of the liquid, σ is the surface tension, a_e is the bubble radius at equilibrium, and κ is the polytropic index of the gas inside the bubble [24].

Assuming that the liquid is incompressible, the scattered pressure at a distance r from the bubble is given by [24]

$$p_{sct}=\frac{a}{r}\left(\frac{1}{2}\rho\dot{a}^2+p_{liq}-p_\infty\right)-\rho\frac{\dot{a}^2a^4}{2r^4}. \quad (2.24)$$

If the driving pressure-bubble volume curve is plotted, the area of a loop in the curve is the energy subtracted from the incident acoustic wave in the time interval corresponding to that loop. The time-dependent nonlinear extinction cross-section of the bubble can be found by dividing the power loss calculated from the driving pressure-bubble volume curve in a specific time interval by the intensity of the driving pressure [20].

2.2 Acoustic Propagation through Bubble Clouds

A bubble cloud changes the sound speed and attenuates the amplitude of an acoustic wave travelling through, in amounts depending on the frequency of the wave. The acoustic wave is scattered by the bubbles and the scattered waves interact with other bubbles. The coherent summation of these scattered waves with phase lags and leads results in an acoustic field with a sound speed fluctuating around a frequency dependent mean sound speed. The scattering of the acoustic wave, the thermal and viscous dissipation at the wall of the bubbles cause the amplitude of the wave to attenuate. The attenuation also fluctuates around a frequency dependent mean attenuation. The fluctuations in the sound speed and attenuation tend to increase as the wave travels through the bubble cloud.

Several theories have been developed modeling the propagation of acoustic waves through bubble clouds. Most of the developed theories are effective medium theories which treat two-phase bubbly mixtures as a single, homogenized medium. Effective medium theories use different approaches like multiple scattering approach, continuum approximation approach, and diagram approach. These theories treat the propagation of acoustic waves through bubble clouds in a statistical sense which is preferable because of the variability inherent in bubble clouds [1].

According to the multiple scattering theory, originally developed by Foldy, a particular configuration of bubbles forms a scattering chain. The pressure field at a point r for an acoustic wave propagating through this scattering chain can be found from the equations:

$$p(r) = p_o(r) + \sum_i s(a_i) p^i(r_i) G(r, r_i) \quad (2.25)$$

$$p^i(r_i) = p_o(r_i) + \sum_{i' \neq i} s(a_{i'}) p^{i'}(r_{i'}) G(r, r_{i'}) \quad (2.26)$$

where p_o is the pressure field in the bubble-free medium, $s(a_i)$ is the scattering coefficient for the i^{th} bubble, $p^i(r_i)$ is the incident pressure at the i^{th} bubble, and $G(r, r_i)$ is the free-space Green's function [1, 30].

The free-space Green's function where r_i is the source point and r is the observation point is written as

$$G(r, r_i) = \frac{e^{-jk|r-r_i|}}{|r-r_i|} . \quad (2.27)$$

For most applications, acoustic wave equation is defined as a linear, hyperbolic, second-order, time-dependent partial differential equation [33]:

$$\nabla^2 p = \frac{1}{c^2} \frac{\partial^2 p}{\partial t^2} . \quad (2.28)$$

If a harmonic solution is assumed for the acoustic pressure, then Eq. (2.28) becomes

$$\nabla^2 p + k^2 p = 0 , \quad (2.29)$$

which is the Helmholtz equation [33].

The following relation holds for the free-space Green's function:

$$\left(\nabla^2 + k_o^2 \right) G(r, r_i) = -4\pi \delta(r - r_i) , \quad (2.30)$$

where k_o is the wavenumber in the bubble-free medium [1].

The average pressure field can be obtained by taking the average of Eq. (2.25) by multiplying it by the joint probability density function of the bubbles in the volume of the bubble cloud interacting with the acoustic wave and integrating over the domains of the random variables [1].

The joint probability density of the bubbles can be written as

$$\rho(r_1, \dots, r_N, a_1, \dots, a_N) , \quad (2.31)$$

where N is the number of the bubbles in the volume of the bubble cloud interacting with the acoustic wave, the random variables r_i and a_i are the position and radius of the i^{th} bubble. If the locations and the sizes of the bubbles are independent, the joint probability density of the bubbles can be written as

$$\rho = (1/N)^N n(r_1, a_1) n(r_2, a_2) \dots n(r_N, a_N) , \quad (2.32)$$

where $n(r_i, a_i)$ is the average number of bubbles per unit volume at position r_i with radius a_i [1].

Assuming that the locations and the sizes of the bubbles are independent and using Eq. (2.25) and Eq. (2.32), the average pressure field is obtained as

$$\langle p(r) \rangle = p_o(r) + \iint_V s_i \langle p^i(r_i) \rangle G(r, r_i) n(r_i, a_i) da_i dr_i . \quad (2.33)$$

Assuming that the acoustic wave is scattered only once by any bubble in the chain, Eq. (2.33) can be written as

$$\langle p(r) \rangle = p_o(r) + \iint_V s_i \langle p(r_i) \rangle G(r, r_i) n(r_i, a_i) da_i dr_i . \quad (2.34)$$

If the Helmholtz operator $(\nabla^2 + k_o^2)$ is applied to both sides of Eq. (2.34), using the relation in Eq. (2.30), the wavenumber k for the bubble cloud medium is found as [1]

$$k^2 = k_o^2 + 4\pi \int sn(r, a) da . \quad (2.35)$$

Expanding the scattering coefficient, Eq. (2.35) becomes

$$k^2 = k_o^2 + 4\pi \int \frac{an(r, a)}{\left(\frac{f_o(a)}{f}\right)^2 - 1 + j\delta(a)} da . \quad (2.36)$$

The effective medium for the bubble cloud is described by the complex wavenumber k . Since amplitude of an acoustic wave propagating through the bubble cloud is proportional to e^{-jk_r} which can be expressed as

$$e^{-jkr} = e^{-j \operatorname{Re}\{k\}r} e^{\operatorname{Im}\{k\}r} , \quad (2.37)$$

the average sound speed and average attenuation coefficient for the bubble cloud as a function of frequency are given as [1]

$$c(f) = \frac{2\pi f}{\operatorname{Re}\{k(f)\}} , \quad (2.38)$$

and

$$\alpha(f) = -\operatorname{Im}\{k(f)\} . \quad (2.39)$$

The pressure field is a random function of position, it can be written as the sum of the average pressure field and the fluctuating pressure field [25]:

$$p(r) = \langle p(r) \rangle + p_f(r) . \quad (2.40)$$

The average field is mentioned as the coherent field and the fluctuating field is mentioned as the incoherent field. The coherent intensity, the incoherent intensity, and the average intensity of the field are defined respectively as [25]:

$$I_c(r) = \left| \langle p(r) \rangle \right|^2 , \quad (2.41)$$

$$I_i(r) = \left\langle \left| p_f(r) \right|^2 \right\rangle , \quad (2.42)$$

$$\langle I(r) \rangle = \left\langle \left| p(r) \right|^2 \right\rangle = I_c(r) + I_i(r) . \quad (2.43)$$

The variance of the pressure field is equal to the incoherent intensity:

$$\sigma_p^2 = \langle pp^* \rangle - \langle p \rangle \langle p^* \rangle . \quad (2.44)$$

Whereas the coherent intensity decays as a result of both scattering and absorption, the average intensity decays as a result of absorption. Hence the coherent intensity decays with range, and the incoherent intensity converges to the average intensity [1].

The variance for a particular configuration of bubbles can be approximately calculated from [1]:

$$\iint_V s_i s_i^* \langle p(r_i) \rangle \langle p^*(r_i) \rangle G_e(r, r_i) G_e^*(r, r_i) n(r_i, a_i) da_i dr_i , \quad (2.45)$$

where G_e is the free-space Green's function for the effective medium.

Eq. (2.25) for the pressure field at a point r for an acoustic wave propagating through the bubble cloud can be expanded as [1]

$$\begin{aligned}
p(r) &= p_o(r) + \sum_i s_i p_o(r_i) G(r, r_i) \\
&+ \sum_{i1 \neq i2} s_{i1} s_{i2} p_o(r_{i2}) G(r_{i1}, r_{i2}) G(r, r_{i1}) \\
&+ \sum_{i1 \neq i2 \neq i3} s_{i1} s_{i2} s_{i3} p_o(r_{i3}) G(r_{i2}, r_{i3}) G(r_{i1}, r_{i2}) G(r, r_{i1}) \\
&+ \dots \\
&= p_o(r) + p_{s1}(r) + p_{s2}(r) + p_{s3}(r) \dots
\end{aligned} \tag{2.46}$$

Using the expansion in Eq. (2.46), the average pressure field can be written as [1]

$$\begin{aligned}
\langle p(r) \rangle &= p_o(r) + \iiint_V s_i p_o(r_i) G(r, r_i) n(r_i, a_i) da_i dr_i \\
&+ \iiint_V s_{i1} s_{i2} p_o(r_{i2}) G(r_{i2}, r_{i1}) G(r, r_{i2}) n(r_{i1}, r_{i2}, a_{i1}, a_{i2}) da_{i1} da_{i2} dr_{i1} dr_{i2} \\
&+ \dots
\end{aligned} \tag{2.47}$$

For a Poisson distributed bubble cloud, the average attenuation coefficient and the average sound speed versus the total number of bubbles estimated using the effective medium theory described by Eqs. (2.36-2.39) are given in Figure 2.1 and Figure 2.2 respectively. The bubble radius is taken as 100 μm and the source frequency is 32.675 kHz.

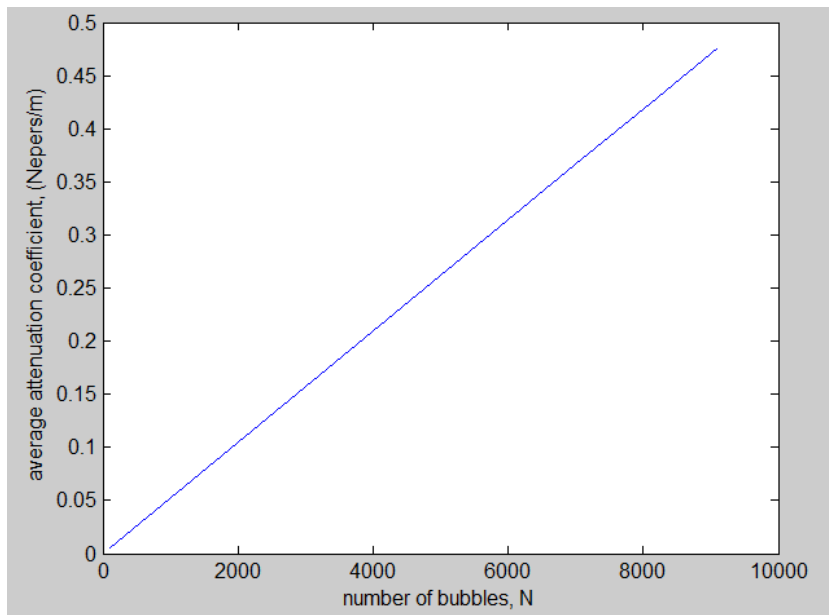


Figure 2.1 Average attenuation coefficient versus number of bubbles.

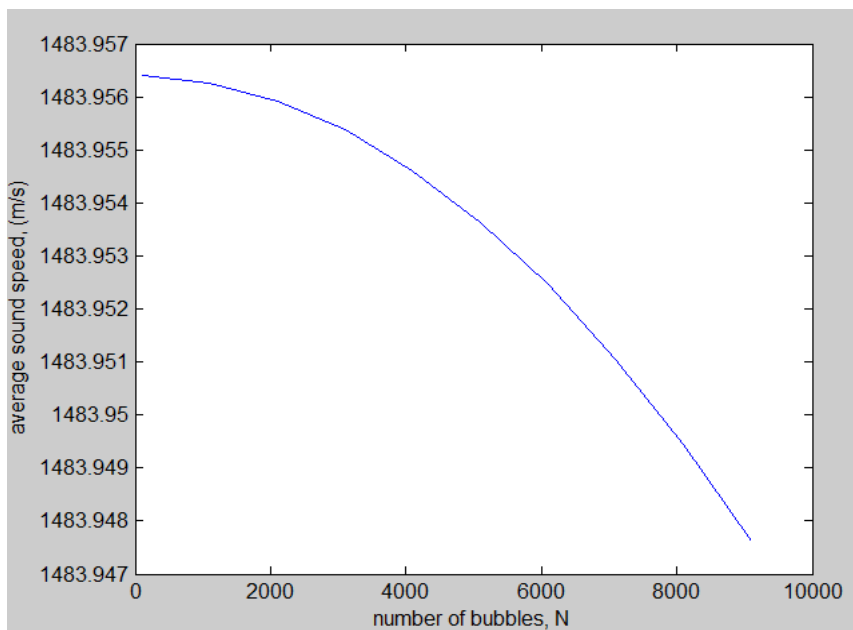


Figure 2.2 Average sound speed versus number of bubbles.

In Figure 2.3 and Figure 2.4, the average attenuation coefficient and the average sound speed versus the source frequency are given respectively. The bubble cloud is Poisson distributed, contains 5000 bubbles with a radius of 100 μm . From Figure 2.3 it can be seen that although the greatest attenuation is near the resonance frequency, there is also a considerable off-resonance contribution to attenuation.

In Figure 2.5 and Figure 2.6, the average attenuation coefficient and the average sound speed versus the source frequency are given respectively for a Gaussian bubble size distribution of 5000 bubbles with a mean radius of 165 μm .

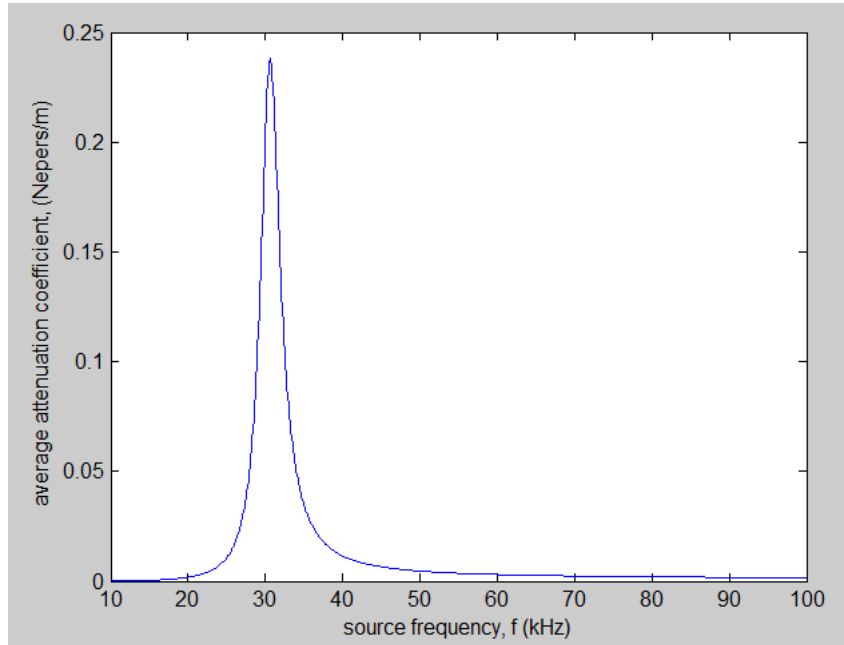


Figure 2.3 Average attenuation coefficient versus source frequency.

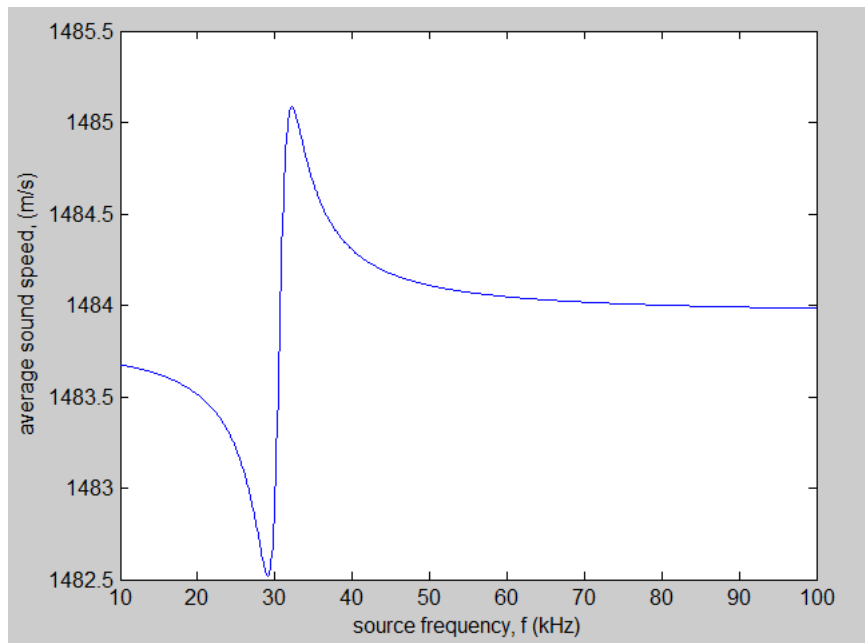


Figure 2.4 Average sound speed versus source frequency.

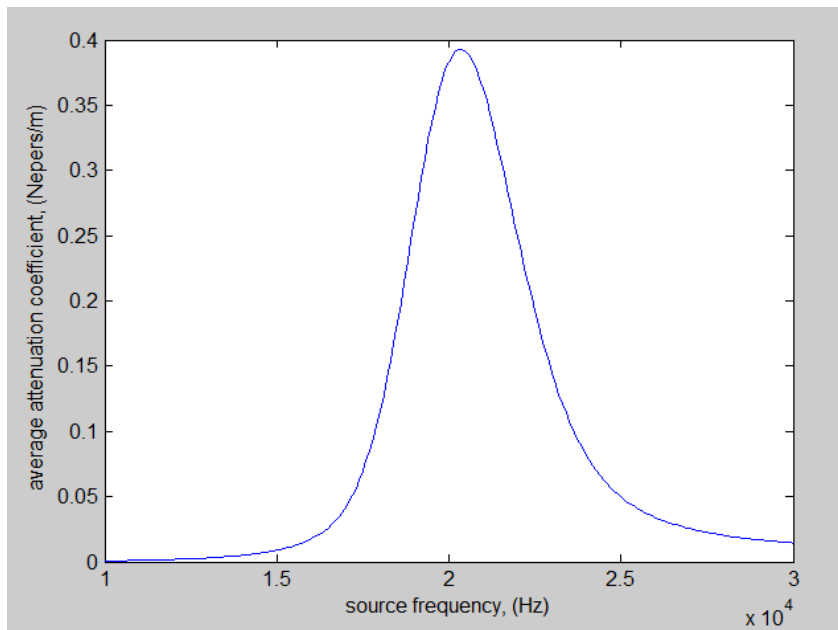


Figure 2.5 Average attenuation coefficient for a Gaussian bubble size distribution.

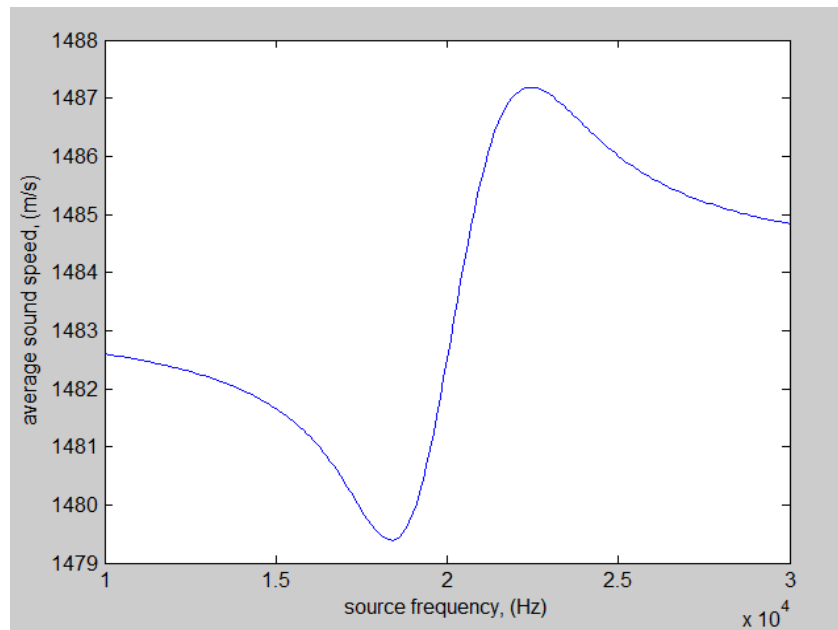


Figure 2.6 Average sound speed for a Gaussian bubble size distribution.

For a Poisson distributed bubble cloud of 1 m^3 containing 500 bubbles of radius $100 \text{ }\mu\text{m}$, the average attenuation coefficient is also estimated using multiple scattering theory described by Eq. (2.46). The attenuation coefficient is calculated from the ratio of the pressure magnitudes at two different locations. The average over 1000 trials is used for the pressure magnitudes. The source frequency is taken as 32.675 kHz. While the average attenuation coefficient considering only single scattering is found as 0.0241, the average attenuation coefficient

considering both single and double scattering is found as 0.0233. The value found from Eq. (2.39) and shown in the graph in Fig. 2.1 is 0.0238.

For clustered bubble clouds, the joint probability density of two bubbles can be written as

$$\rho = (1/N)^2 g(|r_1 - r_2|) n(r_1, a_1) n(r_2, a_2) , \quad (2.48)$$

where $g(|r_1 - r_2|)$ is the pair correlation function of the bubble pair. For uncorrelated bubble pairs, its value can be taken as one [1, 41].

For clustered bubble clouds in which not only single scattering but also double scattering is effective, but triple scattering is negligible, Eq. (2.47) can be written as [1, 41]

$$\begin{aligned} \langle p(r) \rangle = & p_o(r) + \int_V s_i p_o(r_i) G(r, r_i) n(r_i, a_i) da_i dr_i \\ & + \int_V \int_V s_{i1} s_{i2} p_o(r_{i2}) G(r_{i2}, r_{i1}) G(r, r_{i2}) g(|r_{i1} - r_{i2}|) n(r_{i1}, a_{i1}) n(r_{i2}, a_{i2}) da_{i1} da_{i2} dr_{i1} dr_{i2} . \end{aligned} \quad (2.49)$$

Using the pair correlation function in calculation of the joint probability density function instead of assuming independent bubble positions gives more accurate results for the average pressure field calculations [1].

Using measurements of average attenuation and sound speed over a range of frequencies, Eq. (2.36) can be inverted to find the bubble size distribution $n(a)$. A simple inverse operator for Eq. (2.36) is not available; hence various methods have been developed that make some assumptions for the inverse calculation [1, 9].

In the resonant bubble approximation, it is assumed that only the resonant bubbles contribute significantly to attenuation, bubble distribution changes slowly about the resonance radius, δ is constant, and surface tension is negligible. Then the bubble size distribution can be found by inverting Eq. (2.36) as

$$n(a) \cong 4.6 \times 10^{-6} f^3 \alpha(f) , \quad (2.50)$$

where $\alpha(f)$ is in dB/m. If the depth is included as a parameter, Eq. (2.50) becomes [9, 10]:

$$n(a) \cong \frac{4.6 \times 10^{-6} f^3 \alpha(f)}{1 + 0.1z} . \quad (2.51)$$

An iterative approach described in [9] can be followed to obtain the bubble size distribution more accurately than the resonant bubble approximation method. The true attenuation is denoted by β_t and the true bubble size distribution by n_t . The

resonant bubble approximation is represented by the operator RBA acting on β , Eq. (2.39) is represented by the operator FT acting on n , and the inverse of FT acting on β , is FT^{-1} . Then the following steps can be tracked to find the bubble size distribution from a given attenuation function over a range of frequencies:

$$\begin{aligned}
n_o &= RBA[\beta_t] \approx FT^{-1}[\beta_t] = n_t, \\
n_\varepsilon &= n_t - n_o, \\
\beta_o &= FT[n_o] = FT[n_t - n_\varepsilon] = \beta_t - FT[n_\varepsilon], \\
n'_o &= RBA[\beta_o] = n_o - RBA[FT[n_\varepsilon]], \\
n'_\varepsilon &= RBA[FT[n_\varepsilon]], \\
n_\varepsilon &\approx n'_\varepsilon = n_o - n'_o, \\
n_t &= n_o + n_\varepsilon \approx n_o + n'_\varepsilon = n_o + (n_o - n'_o) = 2n_o - n'_o. \quad (2.52)
\end{aligned}$$

In [18, 20], a nonlinear model is used for calculating attenuation and sound speed through bubble clouds. For inversion to estimate the bubble size distribution, it is assumed that the bubble cloud is homogeneous and bubbles are oscillating in steady state.

The bubble cloud volume is the sum of the water volume and the gas volume:

$$V_c = V_w + V_g, \quad (2.53)$$

and from mass conservation:

$$\rho_c V_c = \rho_w V_w + \rho_g V_g. \quad (2.54)$$

The bulk modulus is defined as [2]:

$$B = -V \frac{dP}{dV}. \quad (2.55)$$

Differentiation of Eq. (2.53) with respect to the applied pressure, the following relation between the bulk moduli is obtained:

$$\frac{1}{B_c} = \frac{V_w}{V_c} \frac{1}{B_w} + \frac{V_g}{V_c} \frac{1}{B_g}. \quad (2.56)$$

If the bubble cloud was not dissipative, the following relation could be written for the sound speed through the bubble cloud:

$$c_c = \sqrt{\frac{B_c}{\rho_c}} . \quad (2.57)$$

For the dissipative bubble cloud the function ξ_c is defined as

$$\xi_c = \sqrt{\frac{B_c}{\rho_c}} = \sqrt{\left(\frac{V_c}{\rho_w V_w + \rho_g V_g} \right) \left(\frac{V_w}{V_c B_w} + \frac{V_g}{V_c B_g} \right)^{-1}} , \quad (2.58)$$

which can be approximated as

$$\xi_c \approx c_w \left(1 + \frac{B_w V_g(t)}{V_c B_g(t)} \right)^{-1/2} , \quad (2.59)$$

under low void fraction conditions. If the inhomogeneous bubble cloud is divided into volume elements in which bubbles are subject to the same pressure change, then for the volume element the function ξ_{cl} is

$$\xi_{cl} \approx c_w \left(1 - \rho_w c_w^2 \sum_{j=1}^J n_j(R_{o_j}) \frac{dV_j(t)}{dP_l(t)} \right)^{-1/2} , \quad (2.60)$$

where $n_j(R_{o_j})$ is the number of bubbles per unit volume with an equilibrium radius of R_{o_j} . The function $dV_j(t)/dP_l(t)$ is found from the appropriate bubble dynamics model.

For a nonlinear lossless bubble cloud, $dV_j(t)/dP_l(t)$ varies throughout the oscillatory cycle and the locus of points in the pressure-volume plane is a line which is not straight. The speed of sound varies throughout the oscillatory cycle and is given by Eq. (2.60). If the bubble cloud is dissipative, the locus of points in the pressure-volume plane forms loops with finite areas. In this case, the speed of sound can be inferred from the spine of the loop [18, 20].

As mentioned before, the area of a loop in the pressure-volume curve is the energy subtracted from the incident acoustic wave in the time interval corresponding to that loop. The time-dependent nonlinear extinction cross-section of the bubble can be found by dividing the power loss calculated from the driving pressure-bubble volume curve in a specific time interval by the intensity of the driving pressure.

In [20], a method of inversion of the measured attenuation over a range of frequencies is described to estimate the bubble size distribution. The attenuation measured at a number of discrete frequencies is given by the matrix representation:

$$\alpha = Kn , \quad (2.61)$$

where n is the bubble size distribution giving the count of bubbles at a number of discrete bubble radii. The elements of the matrix K are defined as

$$K_{qj} = \int_0^{\infty} \Omega_b^{ext}(w_q, R_{oj}) B_j(R_{oj}) dR_o , \quad (2.62)$$

where $B_j(R_{oj})$ is the j^{th} spline function for the representation of the continuous bubble size distribution, and $\Omega_b^{ext}(w_q, R_{oj})$ is the extinction cross-section of a bubble with radius R_{oj} when the driving frequency is w_q . In equation Eq. (2.62), the nonlinear cross-sections calculated from the pressure-volume curves of the bubble are used.

For finding the bubble size distribution, a simple matrix inversion for Eq. (2.61) cannot be used. Optimum distribution is given by the expression

$$n_{opt} = (K^T K + \beta I)^{-1} (K^T \alpha) , \quad (2.63)$$

where β is the regularization parameter [20].

2.3 Backscattering and Target Strength of Bubble Clouds

For a mono-static configuration of the source and the receiver, namely the locations of the source and the receiver being the same, the backscattered pressure signal $p(r)$ received at the receiver from the portion of a bubble cloud containing N bubbles insonified by a source pressure signal can be written as

$$p(r) = \sum_{i=1}^N p_o(r_i) s(a_i) G(r, r_i) , \quad (2.64)$$

assuming only single scattering is important [1].

The pair correlation function, showing the clustering in the bubble cloud can be found from correlation of the backscattered pressure signals from different locations of the bubble cloud. Correlation between backscattered pressure from two different locations can be written as

$$\langle p_1(r) p_2(r) \rangle = \int \int \int \int_V s(a_i) s(a_j) p_o(r_i) p_o(r_j) G(r, r_i) G(r, r_j) n(a_i, a_j, r_i, r_j) da_i da_j dr_i dr_j . \quad (2.65)$$

Using Eq. (2.48), Eq. (2.65) can be rewritten as

$$\langle p_1(r)p_2(r) \rangle = \int_V \int_V \int s(a_i)s(a_j)p_o(r_i)p_o(r_j)G(r, r_i)G(r, r_j)g(|r_i - r_j|)n(a_i, r_i)n(a_j, r_j)da_ida_jdr_idr_j \quad (2.66)$$

Assuming that the pair correlation function is independent of position, the following expression can be written from Eq. (2.66):

$$g(d) = \frac{\langle p_1(r)p_2(r) \rangle}{\langle p_1(r) \rangle \langle p_2(r) \rangle}, \quad (2.67)$$

where d is the distance between the considered backscattering locations of the bubble cloud [1].

For an active sonar signal with pulse shape $x(t)$ and spectrum $X(f)$, the received signal, namely the echo from the insonified portion of the bubble cloud can be written as

$$y(t) = \int_{f=-\infty}^{\infty} \sum_{i=1}^N X(f)s(a_i)H(r_i, r)G(r, r_i)e^{-j2\pi ft} df. \quad (2.68)$$

The received spectrum is [12, 17]

$$Y(f) = \sum_{i=1}^N X(f)s(a_i)H(r_i, r)G(r, r_i). \quad (2.69)$$

Signal processing like matched filtering can be applied on this received signal for a better discrimination of the bubble cloud.

The target strength TS of an underwater target refers to the magnitude of the echo from the target. It is defined as:

$$TS = 10 \log \frac{I_r}{I_i}, \quad (2.70)$$

where I_i is the incident intensity and I_r is the reflected intensity referred to 1 m from the center of the target [27].

If V is the insonified volume of the bubble cloud and S_s is the scattering cross-section per unit volume, then the target strength can be written as [3]:

$$TS = 10 \log \left(\frac{S_s}{4\pi} V \right). \quad (2.71)$$

The scattering cross-section per unit volume is [3]:

$$S_s = \int_0^{\infty} \sigma_s n(a) da = \int_0^{\infty} \frac{4\pi a^2 n(a) da}{\left(\frac{w_o^2}{w^2} - 1\right)^2 + \delta^2} . \quad (2.72)$$

For a mono-static configuration of the source and the receiver, the active sonar equation can be written as:

$$RL = SL + TS - 2TL - 2TL_b , \quad (2.73)$$

where RL is the receive level, SL is the source level, TL is the one-way transmission loss, and TL_b is the one-way transmission loss caused by the bubble cloud.

Transmission loss is given as

$$TL = 10 \log \left(\frac{I_o}{I_r} \right) , \quad (2.74)$$

where I_o is the intensity at the initial point and I_r is the intensity at the arrival point [27]. It can be written as the sum of spreading loss and absorption loss:

$$TL = 20 \log r + \alpha r \times 10^{-3} , \quad (2.75)$$

where r is the distance travelled in meters, and α is the attenuation coefficient due to absorption in dB/km.

Transmission loss caused by the bubble cloud is given as

$$TL_b = 4.34 \times S_e \times r , \quad (2.76)$$

where extinction cross-section per unit volume of the bubble cloud is

$$S_e = \int_0^{\infty} \sigma_e n(a) da = \int_0^{\infty} \frac{4\pi a^2 (\delta / ka) n(a) da}{\left(\frac{w_o^2}{w^2} - 1\right)^2 + \delta^2} . \quad (2.77)$$

In [3], an iterative technique has been described for estimating the bubble size distribution from measurements of receive level for different source frequencies. Using Eq. (2.72) and Eq. (2.73), the scattering cross-section per unit volume can be expressed as:

$$10 \log S_s = RL - SL + 2TL_b + 2TL - 10 \log V + 10 \log 4\pi . \quad (2.78)$$

For the different source frequencies, Eq. (2.69) is expressed as:

$$S_s^{fi} = \int_0^{\infty} \sigma_s^{fi} n(a) da , \quad (2.79)$$

and an initial guess is made for $n(a)$. Using this initial guess for the bubble size distribution, Eq. (2.79) is calculated for the different source frequencies used in the measurements. Calculated scattering cross-section values are compared with the ones found from Eq. (2.78) and the bubble size distribution $n(a)$ is adjusted accordingly.

CHAPTER 3

SHIP WAKE ECHO

3.1 Ship Wake Structure

Ships generate bubbles by propeller cavitation, by breaking of ship generated waves, and by air entrapment in the turbulent boundary layer under the ship hull [6]. As bubbles breakup, turbulent diffusion causes bubbles to mix and fragment. Afterwards, turbulence decays and the bubbles of different sizes begin to rise at different rates towards the surface due to their buoyancy. The main physical processes affecting the bubbles in this phase are advection by local currents, turbulent diffusion, buoyant degassing, and dissolution [1, 29]. Ship propeller and hull design, ship speed and maneuver affect the bubble distribution and hence wake signature [6, 10, 15].

In literature it is possible to find various experimental and theoretical work related to modeling the ship wake structure [6, 7, 10, 15, 16, 17, 26, 29, 68, 71, 90, 100, 102, 103, 117, 125]. On the other hand, a complete model of the ship wake structure that includes the initial bubble distribution and the evolution of the bubble distribution in relation with the ship and ambient parameters does not exist in the open literature.

In various experiments, it has been observed that ship wakes could last for about 15 minutes [1, 15]. Usual values for ship wake length, depth and width are approximately 1500 m, 10 m, and 30 m respectively. Commonly, wake depth is 2 times the ship's draft and width is 5 to 10 times the ship's beam [15]. Actually, ship wake can be modeled as being composed of a central wake formed by propellers and the hull, and left and right wakes caused by the bow waves [17].

It is common to represent mean bubble density in the ship wake as a function of bubble radius with power law or quadratic equations. Using power law, mean bubble density can be written as

$$n(a) \propto a^{-s} , \quad (3.1)$$

where s takes values between 2.5 and 4 [6, 10, 102].

In [102], a ship wake model is formed for acoustic propagation studies. In this model, the mean bubble density profile of the ship wake is constructed from the data found in the literature. A separate stochastic function is used to form the random structure of the bubble density.

The mean bubble density $N(x, y, z, a)$, namely the mean number of bubbles per m^3 at location (x, y, z) with radii between a and $a + da$ is written as

$$N(x, y, z, a) = N_x(x).N_y(y).N_z(z).A(a) \quad (3.2)$$

where $N_x(x)$, $N_y(y)$, and $N_z(z)$ are separable functions giving the x, y, and z axes (range, cross range, and depth axes) dependence of the bubble density and $A(a)$ is the bubble size distribution. In Figure 3.1, the representation of wake range, wake cross range, and wake depth axes is given.

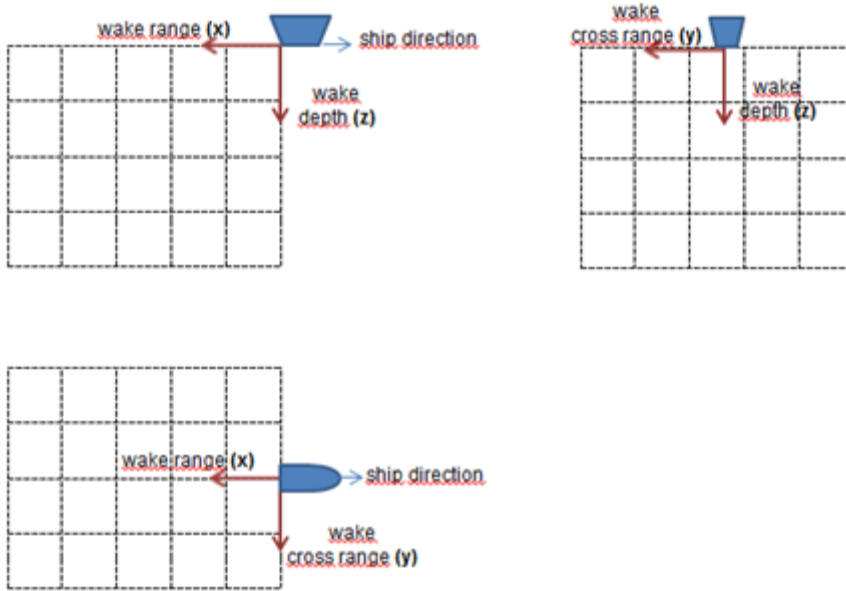


Figure 3.1 Representation of wake axes.

The void fraction $u(a)$ is defined as the volume of air per m^3 formed by bubbles with radii between a and $a + da$ and written as

$$u(a) = \left(\frac{4}{3} \pi a^3 \right) N(a) . \quad (3.3)$$

The bubble size distribution is given as

$$A(a) = a^{-4} \quad (3.4)$$

for bubble radii between $50 \mu\text{m}$ and $1000 \mu\text{m}$.

Along-wake dependence of the bubble density is given as

$$N_x(x) = 10^{(-3.10^{-3}) \left(\frac{x}{v} \right) - 13.3} , \quad (3.5)$$

where v is the speed of the ship.

Cross-wake dependence of the bubble density is given as

$$N_y(y) = e^{-(y/\sigma)^2}, \quad (3.6)$$

where the parameter σ depends on the distance astern.

Depth dependence of the bubble density is given as

$$N_z(z) = N_z(z=0).e^{-\left(\frac{z}{D/coeff2}\right)}, \quad (3.7)$$

where the parameter D defined as the characteristic depth of the wake depends on the distance astern. Varying the constant parameter $coeff2$ forms a deeper or shallower wake.

In order to randomize the wake profile defined by Eq. (3.2), the following steps are applied: A zero-mean Gaussian distribution is formed with unit variance for along-wake and cross-wake axes. The desired correlation of the field in x and y directions is obtained by convolving the field in x and y directions by a suitable kernel. This field referred as $corr(x, y)$ is scaled by the constant parameter $coeff1$ for adjusting the variance of the field and the field is biased to make the center value unity. The resultant field is used to scale both $N_z(z)$ and the parameter D in Eq. (3.7) to obtain $N_{z,rand}(x, y, z)$ which replaces $N_z(z)$ in Eq. (3.2):

$$N_{z,rand}(x, y, z) = (coeff1.corr(x, y) + 1).N_z(z=0).e^{-\left(\frac{z}{(coeff1.corr(x, y)+1).D/coeff2}\right)}. \quad (3.8)$$

In Figure 3.2, bubble density profile of the wake obtained by simulating the model in [102] is given. The locations of the yz -plane, xz -plane, and xy -plane are at $x=650$ m, $y=6$ m, and $z=2$ m respectively. The bubble density profile is for a bubble radius of $160 \mu\text{m}$. The following values are used for the parameters:

$$\sigma(t) = [12.5, 12.1, 12.6, 15.7, 17.1, 19.1, 30] \text{ m},$$

$$D(t) = [7.4, 8.3, 9.0, 7.0, 5.3, 2.5, 1.3] \text{ m},$$

$$t = [75, 125, 175, 225, 275, 325, 375] \text{ s},$$

$$v = 7.5 \text{ m/s},$$

$$coeff2 = 2.3,$$

$$coeff1 = 1.5,$$

$$\text{kernel dimension for } corr(x, y) = [10, 10]. \quad (3.9)$$

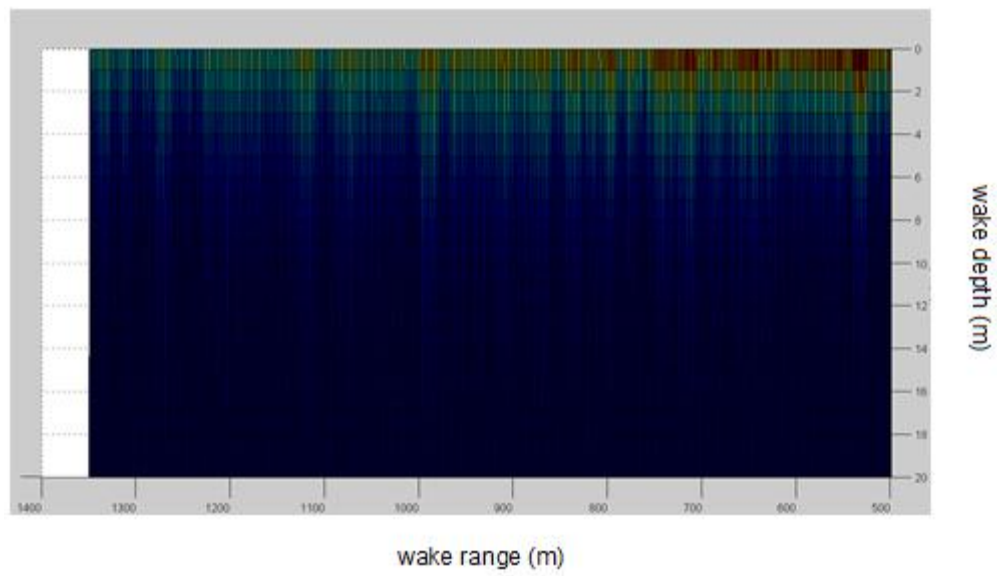
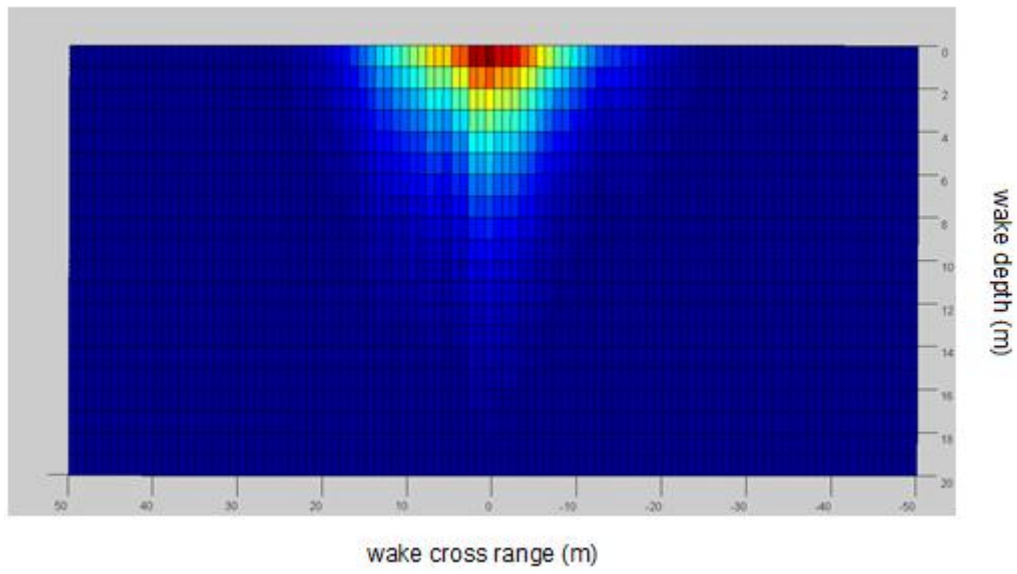


Figure 3.2 Bubble density profile of the simulated wake.

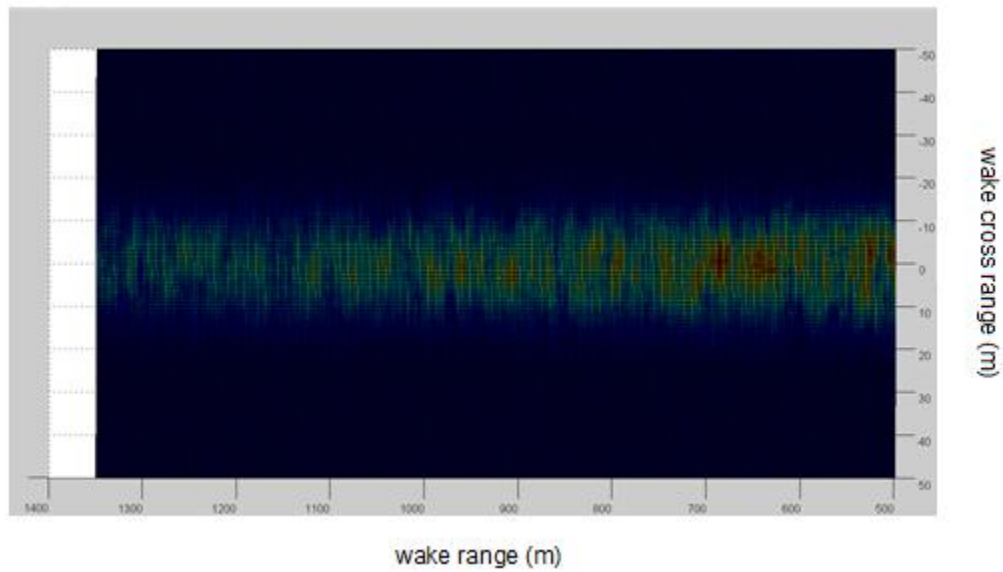


Figure 3.2 (continued).

For the mean bubble density profile, namely for $coeff1=0$, void fraction values and bubble density values at different wake ranges and for different bubble radii are given in Table 3.1. Depth and cross range values are taken as 3 m and 6 m respectively.

Table 3.1 Void fraction and bubble density values

Bubble radius (μm)	Distance (m)	Void fraction w.r.t. bubble density	Bubble density ($\#/\text{m}^3/\mu\text{m}$)
160	500	$3.26 \cdot 10^{-10}$	19.00
160	1000	$2.30 \cdot 10^{-10}$	13.41
400	500	$1.30 \cdot 10^{-10}$	0.49
400	1000	$0.92 \cdot 10^{-10}$	0.34

More complex wake models have also been constructed in the literature. In a recent work [103], it is stated that the wake of a ship is governed by the water current pattern in the wake. Bubbles are distributed in the water by the wake

currents. Besides the acoustic signature created by the bubbles, the currents in the wake can also create an acoustic signature.

In [103], two different wake models are investigated. Given an initial condition just behind the ship, these models describe the evolution of the far field wake currents. The Swanson model is intended for flows created by the movement of the hull of the ship through the water and the Chernykh-Loitsyanskiy model is intended for flows created by the propeller of the ship.

In the Swanson model, the width of the axial wake b is expressed as the result of the contributions of ship turbulence, wake turbulence, and ambient turbulence:

$$b = d \sqrt{0.2966(x/d)^{8/15} + 2fc_D(x/d) + 10^{2f_t} 1.348 \cdot 10^{-7} d^{6/17} (x/Ud)^{40/17} + 3.4}, \quad (3.10)$$

where d is the ship beam, U is the ship speed, f is the ratio of wave drag to total drag, and c_D is the total drag coefficient.

The axial (x-direction) velocity of the wake current is given as:

$$V_x(x, y, z) = \frac{0.5fc_D U d h}{b(x)h\sqrt{\pi}} \exp\left(-\left(\frac{y}{b}\right)^2\right) \exp\left(-\frac{\pi}{4}\left(\frac{z}{h}\right)^2\right), \quad (3.11)$$

where h is the ship draft. Eq. (3.11) is found by equating the amount of axial momentum in the wake to the momentum radiated forward by the ship and assuming a Gaussian profile for the cross wake and vertical directions.

A vortex pair is defined behind the ship. A mirrored virtual vortex pair above the water is assumed to model the free surface condition. The y-direction and z-direction velocities of the wake current are given by the sum of the contributions of these four vortices. A vortex is described by a circulation Γ :

$$\Gamma = 2\pi V_t(r), \quad (3.12)$$

where $V_t(r)$ is the tangential velocity due to the vortex at a distance r from the vortex center.

The circulation decays with time and the depth of the vortices Z_v and the separation between them b_v change with time. The initial value of the circulation is given as

$$\Gamma_0 = \frac{c_p U l}{2f_h} \quad (3.13)$$

at

$$t_0 = \frac{2\pi(f_h d / 2)^2}{\Gamma_0}, \quad (3.14)$$

where l is the ship length, f_h is the ship hull form factor, and the parameter c_p is defined as

$$c_p = 1.5 \left(\frac{d}{l} \right)^{3/2} . \quad (3.15)$$

The circulation $\Gamma(\tau)$ can be expressed as

$$\Gamma(\tau) = \Gamma_0 \frac{dG(\tau)}{d\tau} , \quad (3.16)$$

with $\tau = t/t_0$ and

$$G(\tau) = \frac{\tau}{\left(1 + \left(\frac{1}{3} (\tau/3)^\beta \right)^p \right)^{1/p}} - 1 , \quad (3.17)$$

with $\beta = 0.598 + 0.396f_t$ and $p = 3.9 - 2.7f_t$ where f_t is the measure of the ambient ocean surface turbulence.

The vortex pair separation is given as

$$b_v = d \left(1 + f_h^2 G(\tau) / 2 \right) , \quad \text{for } f_t = 0 \quad (3.18)$$

$$b_v = d \left(1 + \left(\sqrt{f_t f_h^2 G(\tau) + 1} - 1 \right) / f_t \right) . \quad \text{for } f_t > 0 \quad (3.19)$$

The depth of the vortex pair is given as

$$Z_v = f_t \frac{b_v}{2} + (1 - f_t) \frac{d}{2} . \quad (3.20)$$

The y-direction and z-direction velocities of the wake current are given as [103, 105]:

$$V_y(x, y, z) = \frac{\Gamma(t)}{2\pi} \left[\frac{z + Z_v}{(y - b_v/2)^2 + (z + Z_v)^2} - \frac{z + Z_v}{(y + b_v/2)^2 + (z + Z_v)^2} + \frac{z - Z_v}{(y + b_v/2)^2 + (z - Z_v)^2} - \frac{z - Z_v}{(y - b_v/2)^2 + (z - Z_v)^2} \right] , \quad (3.21)$$

$$V_z(x, y, z) = \frac{\Gamma(t)}{2\pi} \left[-\frac{y-b_v/2}{(y-b_v/2)^2 + (z+Z_v)^2} + \frac{y+b_v/2}{(y+b_v/2)^2 + (z+Z_v)^2} - \frac{y+b_v/2}{(y+b_v/2)^2 + (z-Z_v)^2} + \frac{y-b_v/2}{(y-b_v/2)^2 + (z-Z_v)^2} \right]. \quad (3.22)$$

In the Chernykh-Loitsyanskiy model, similar to the Swanson model, the velocity field of the wake is formed as the summation of the velocity fields of four vortices behind the ship. The axial, radial, and tangential velocity components for a single vortex field are given as:

$$U(r, x) = \frac{2\alpha^2}{\left(1 + \frac{1}{4}\alpha^2\eta^2\right)^2} \frac{1}{x}, \quad (3.23)$$

$$V(r, x) = \frac{\sqrt{\nu}\eta\alpha^2\left(1 - \frac{1}{4}\alpha^2\eta^2\right)}{\left(1 + \frac{1}{4}\alpha^2\eta^2\right)^2} \frac{1}{x}, \quad (3.24)$$

$$W(r, x) = \frac{\gamma\alpha\eta}{\left(1 + \frac{1}{4}\alpha^2\eta^2\right)^2} \frac{1}{x}, \quad (3.25)$$

where $\alpha = \sqrt{3J_0/16\pi\mu}$, $\gamma = (3\sqrt{3}/64\pi\sqrt{\pi})(L_0\sqrt{\rho J_0}/\mu^2)$, $\eta = r/x\sqrt{\nu}$, and $\mu = \rho\nu$, with $\rho = 1000 \text{ g/cm}^3$, $\nu = 0.05e-4 \text{ cm}^2/\text{s}$, $J_0 = 0.01 \text{ g/cm}^2$, $L_0 = 0.01 \text{ g/cm}^2$, and $\beta = 2.5 \text{ cm.s/g}$.

The x, y, and z direction velocity components can be found from:

$$V_x(r, x) = U(r, x), \quad (3.26)$$

$$V_y(r, x, \varphi) = V(r, x)\cos(\varphi) - W(r, x)\sin(\varphi), \quad (3.27)$$

$$V_z(r, x, \varphi) = V(r, x)\sin(\varphi) + W(r, x)\cos(\varphi), \quad (3.28)$$

with $r = \sqrt{y^2 + z^2}$ and $\varphi = \tan^{-1}(z/y)$.

In [103], the initial distribution of the wake bubbles behind the ship is modeled as

$$P(x) = N \frac{e^{(a-x)/b} - e^{(a-x)/b}}{b}, \quad (3.29)$$

with $a = 2$, $b = 1$, and $x = (7/400)R$, where R is the bubble radius and N is the number of bubbles. It is mentioned that this model is just an assumption.

The terminal rise velocity of the bubbles (in cm/s) is

$$V_t = -0.417 + 0.0112 \cdot (2R) + 1.42 \cdot 10^{-6} \cdot (2R)^2 \quad (3.30)$$

which is added to the V_z component of the velocity field of the wake.

When a bubble rises, because of the pressure decrease, the volume of the bubble increases and the radius change is given by:

$$\Delta R_{rise} = \left(\frac{3 \left(1 - \frac{z_{n-1}}{10} \right) \left(\frac{4}{3} \pi R_{n-1}^3 \right)}{4 \pi \left(1 - \frac{z_n}{10} \right)} \right)^{1/3} - R_{n-1} \quad (3.31)$$

The radius change of bubbles due to dissolution is given as

$$\Delta R_{diss} = -10^{-6} \Delta t \quad (3.32)$$

The bubble distribution in the wake of a ship is simulated in [103] by using this initial bubble distribution and bubble evolution model and the wake current models.

Since the mean bubble density profile of the wake model in [102] depends on data found in the literature, it is supposed that the wake model will give realistic and sufficient results for the studies related to this thesis. Besides, the model and the parameters involved are simple to implement and interpret. Hence, the wake model described in [102] will be taken as the basis for the wake profiles used in this thesis.

In this thesis, the wake model in [102] is used with some modifications. The bubble radius is taken to be between 50 μm and 400 μm . It is known that small sized bubbles last for a longer time than bigger sized bubbles. Hence, again Eq. (3.2) is used for bubble density, but for each 100 m of the wake, it is assumed that only the bubbles with radii indicated in Table 3.2 could exist and Eq. (3.2) is scaled by a factor of 10.

Table 3.2 Bubble size distribution

Wake range (m)	Bubble radius (μm)
0-100	150-400
100-200	140-350
200-300	120-300
300-400	100-250
400-500	80-200
500-1000	50-200
1000-1500	50-150

In order to model the wake starting from the beginning of the wake range, namely starting from $t = 0$ s, the values of the parameters in Eq. (3.9) are extended as

$$\begin{aligned}\sigma(t) &= [3, 7, 9, 12.5, 12.1, 12.6, 15.7, 17.1, 19.1, 30] \text{ m}, \\ D(t) &= [1, 3, 5, 7.4, 8.3, 9.0, 7.0, 5.3, 2.5, 1.3] \text{ m}, \\ t &= [0, 25, 50, 75, 125, 175, 225, 275, 325, 375] \text{ s}.\end{aligned}\tag{3.33}$$

3.2 Ship Wake Echo

The wake model in [102] with modifications indicated in Section 3.1 is used to simulate the receive level profile when insonifying a ship wake. The values in Eq. (3.33) and Eq. (3.9) are used for the parameters of the bubble density equation given by Eq. (3.2). The bubble radius is taken to be between 50 μm and 400 μm as in Table 3.1. The maximum depth of the wake is taken as 20 m, the maximum width of it as 100 m, and the length of it as 1500 m.

The wake is divided into cells having dimensions of 100 m in range, 1 m in cross range, and 1 m in depth. It is assumed that the bubble density in each cell is uniform and found by taking the average of the bubble densities corresponding to 1 m^3 portions of the cell.

The receive level for each cell is calculated using Eq. (2.73) with the source frequency and pressure being 30 kHz and 300 kPa respectively. The scattering cross-section per unit volume and the extinction cross-section per unit volume of the cells are found using Eq (2.72) and Eq. (2.77). Corresponding target strength and attenuation coefficient of the cells are found using Eq (2.71) and Eq. (2.76).

For the figures below; the range, width, and depth of the wake corresponds to the x-axis, y-axis, and z-axis respectively. In Figure 3.4, the receive level profile for the x-y plane of the wake at 1 m of depth when insonifying each wake cell from the side of the wake is given. For each cell, the source-receiver pair is brought to the same range as the middle point of the cell and 500 m away from $y=0$ m, and 1 m depth. The diagram showing the measurement scenario is given in Figure 3.3. Since the receive level is in dB scale and its interval is large, different receive levels are not easily distinguished in Figure 3.4.

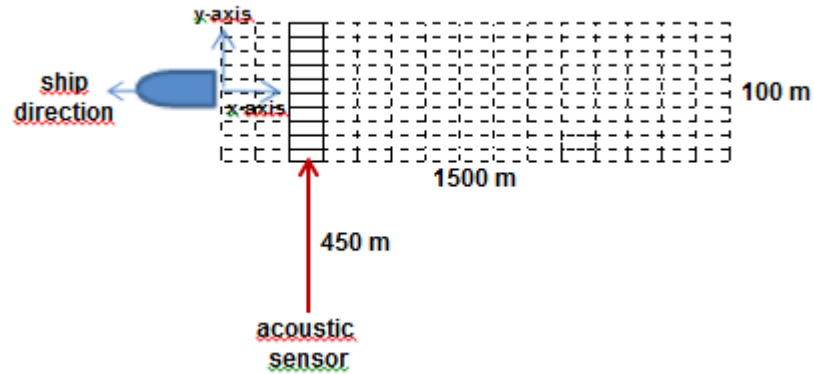


Figure 3.3 Receive level profile measurement scenario.

In Figure 3.5, a background Gaussian noise with a mean of 20 dB and a standard deviation of 6 dB is added to the receive level profile of Figure 3.4. It can be seen that due to the attenuation caused by the bubbles, the receive level obtained from the distant half of the wake with respect to the source is lower than the near half of the wake.

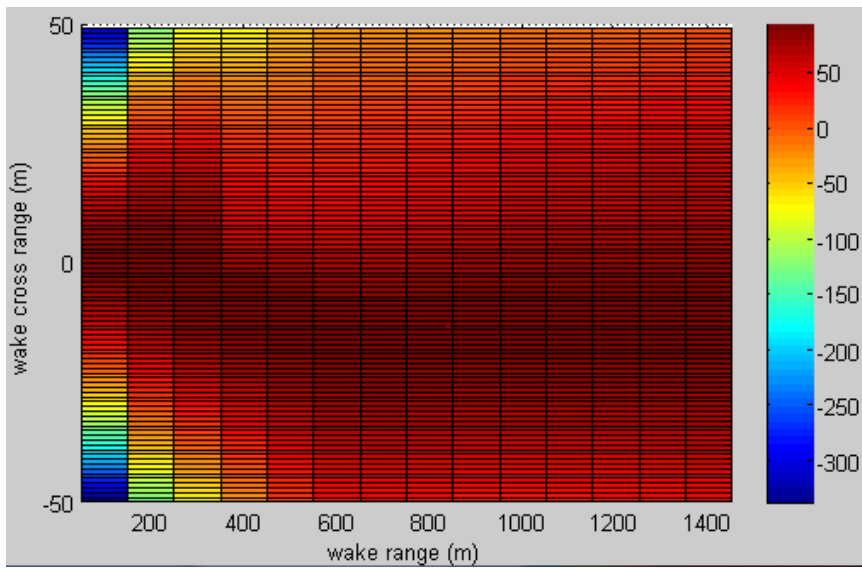


Figure 3.4 Receive level profile when insonifying the wake from the side.

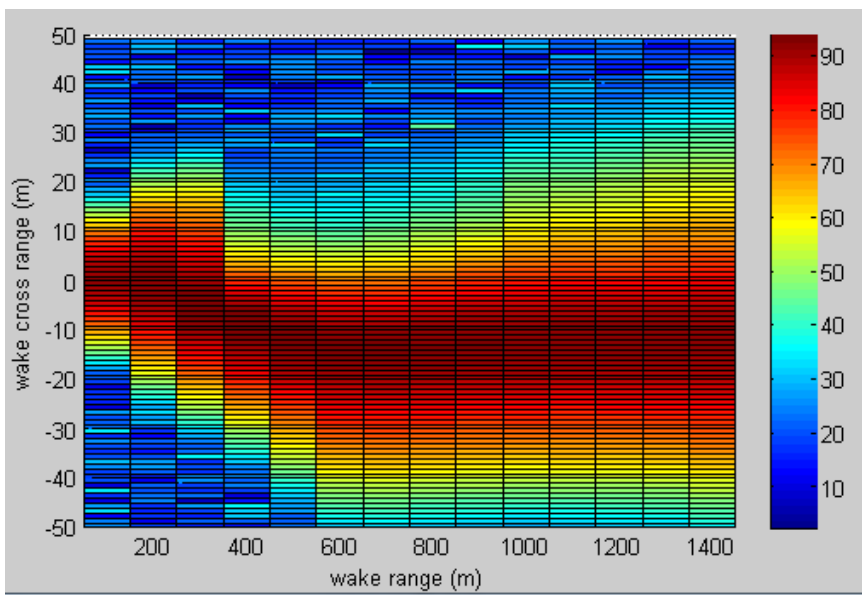


Figure 3.5 Receive level profile when insonifying the wake from the side with background noise added.

CHAPTER 4

ACOUSTIC DETECTION AND TRACKING OF SHIP WAKES

4.1 Introduction

For acoustic detection and tracking of targets, a large literature exists. When the target is a ship wake, various features of the ship wake could be exploited for acoustic detection and tracking.

In [66], an automatic detection and tracking algorithm is described to detect and track a ship based on the evolution of its wake observed in the sonar image sequence. The strong noise created by propeller cavitation is used to estimate the bearing of the starting point of the wake. Then a linear feature corresponding to the wake is determined from the range measurements at the estimated target bearing. Range normalization and clutter map processing are used to reduce the number of false measurements. Kalman filter is used for tracking.

In literature [18], exploiting the nonlinear dynamics of the bubbles stands out as a promising method for detecting ship wakes. The insonifying signal could be adjusted such that while linear scatterers give little or no response, response from ship wake bubbles is high enough for detection.

There are also papers [17] dealing with modelling the echo signals of ship wakes insonified by an active sonar. Matched filter and energy detector are among the detectors used on the echo time series. The effect of parameters such as distance to the ship, the aspect angle, and the source frequency is investigated using the echo models developed.

In Section 4.2, some features of the ship wake echo level pattern that could be exploited for detection and tracking will be outlined. The echo level pattern of the ship wake model explained in Chapter 3 will be investigated for this purpose.

In Section 4.3, particle filter method will be used for tracking instead of using Kalman filter method, since wake echo measurement is a nonlinear function of target position.

4.2 Wake Features for Detection and Tracking

Ship wake has a complex pattern formed by the processes explained in Chapter 3. It is proposed that various features of this pattern could be exploited for detection and tracking. Simulations have been carried out using the ship wake model mentioned in Chapter 3 to figure out the ship wake echo patterns for different conditions. Features of the ship wake echo level pattern that could be exploited for detection and tracking are outlined.

In Chapter 3, it was mentioned that due to the attenuation caused by the bubbles, when insonifying the wake from the side, the receive level obtained from the distant half of the wake with respect to the source is lower than the near half of the wake. This property of the ship wake is evident when insonifying the wake with frequencies near to resonant frequencies of bubbles.

In Figure 4.2, the receive levels of Figure 3.5 with 30 kHz source frequency are summed along the wake range and the result is plotted against the wake cross range.

It can be seen that the resulting plot is non-symmetric and its peak is near -10 m instead of 0 m. The same plot is repeated with different source frequencies and the results are given in Figure 4.2. The measurement configuration is shown in Figure 4.1. Also, in Figure 4.3 receive level at 600 m wake range and 1 m depth obtained with different source frequencies are given.

For different source frequencies, the plots become more or less symmetric depending on the bubble size distribution of the wake portion insonified. This feature of ship wakes could be a distinctive property for detection.

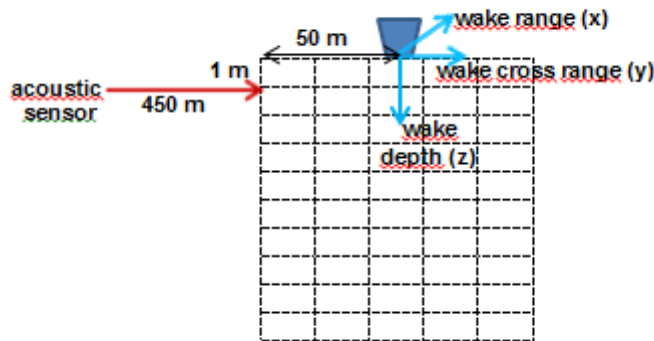


Figure 4.1 Measurement configuration for receive level summation.

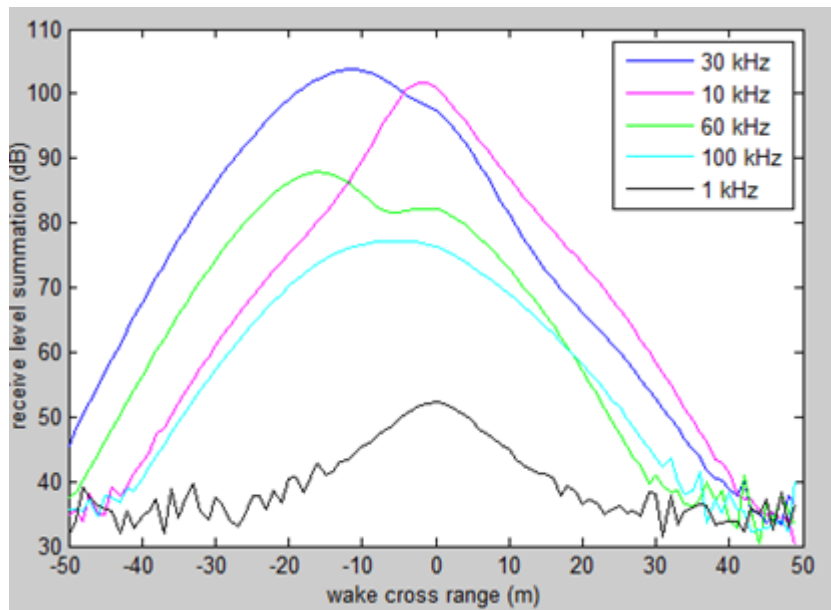


Figure 4.2 Receive level summation along the wake range at 1 m depth.

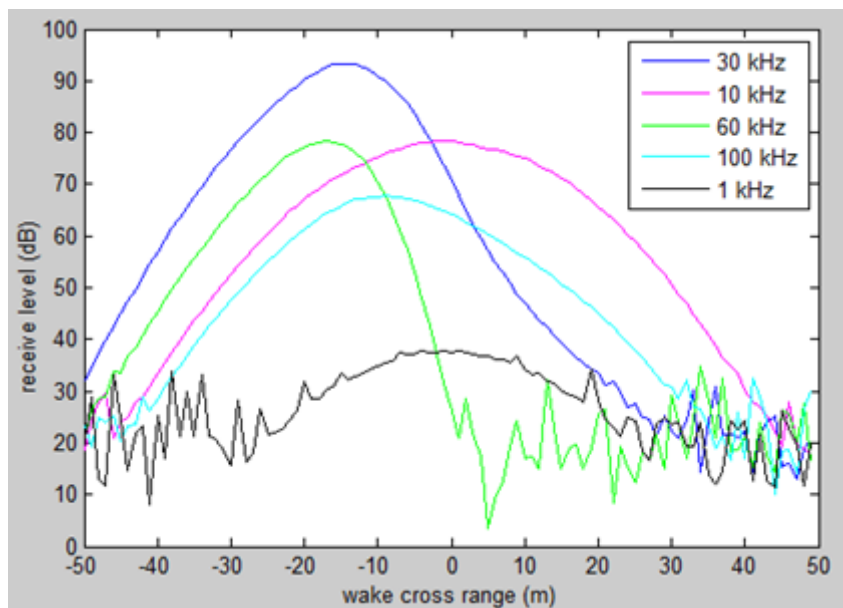


Figure 4.3 Receive level at 600 m wake range and 1 m depth.

Since ship wakes contain various sizes of bubbles, the target strength and hence the echo level of the wake cells change with source frequency. In Figure 4.4, Figure 4.5, Figure 4.6, and Figure 4.7, the receive levels obtained with source frequencies of 1 kHz, 10 kHz, 30 kHz, and 200 kHz are given respectively. The wake is insonified from the side with the source and receiver located at the same range as middle point of each cell and 500 m away from $y=0$ m, and at 1 m depth. Background noise is Gaussian with a mean of 20 dB and a standard deviation of 6 dB. The measurement configuration is as in Figure 3.3.

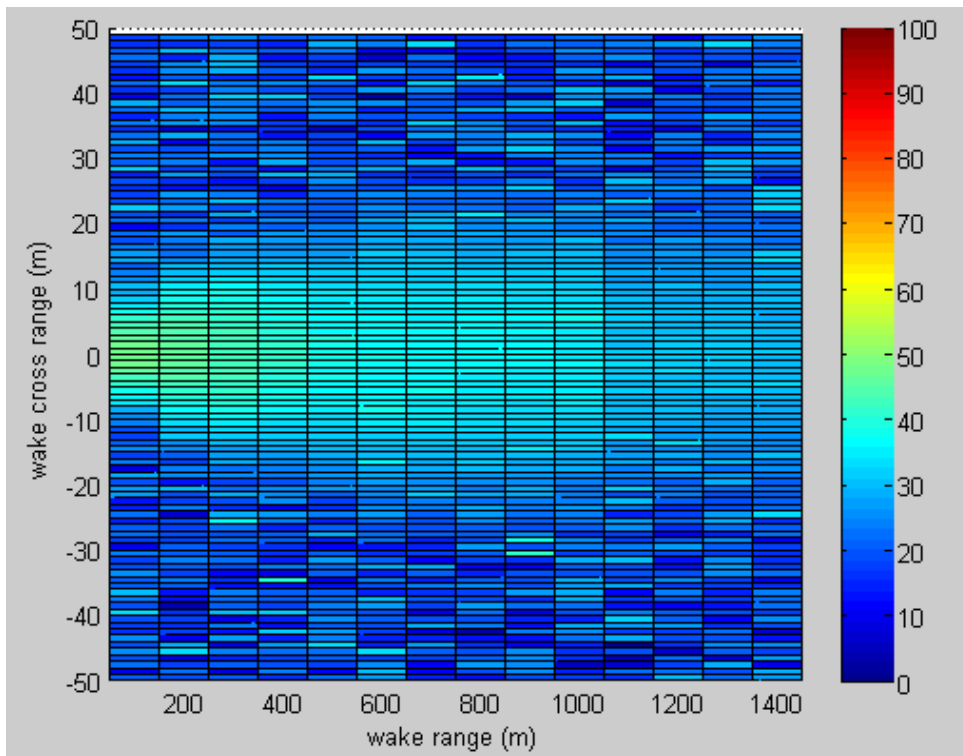


Figure 4.4 Receive level profile with 1 kHz source.

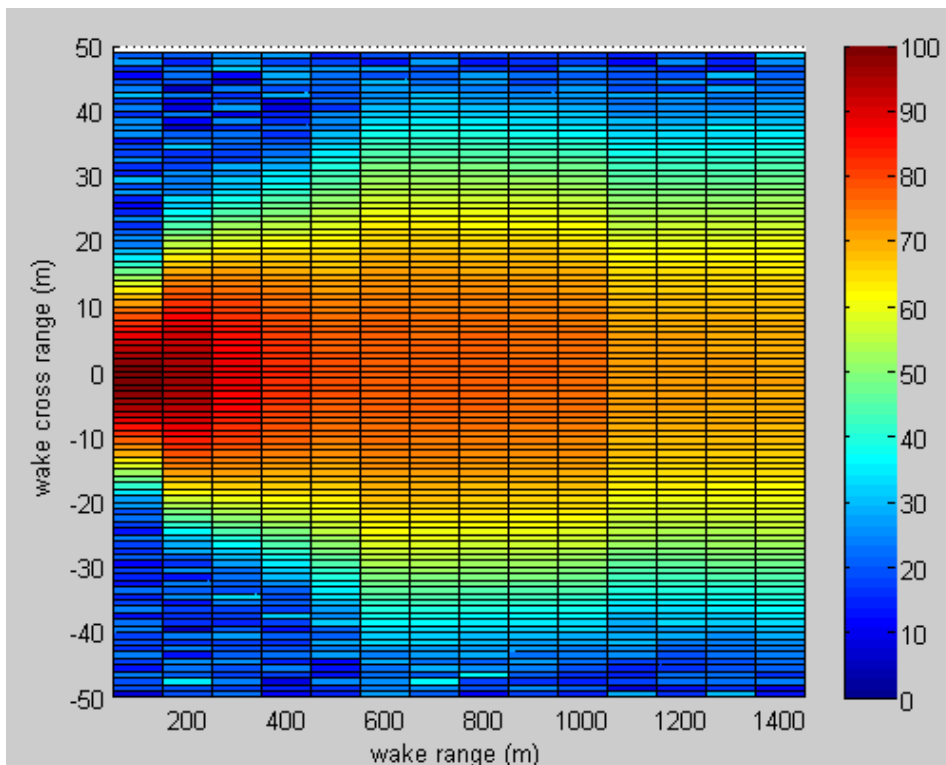


Figure 4.5 Receive level profile with 10 kHz source.

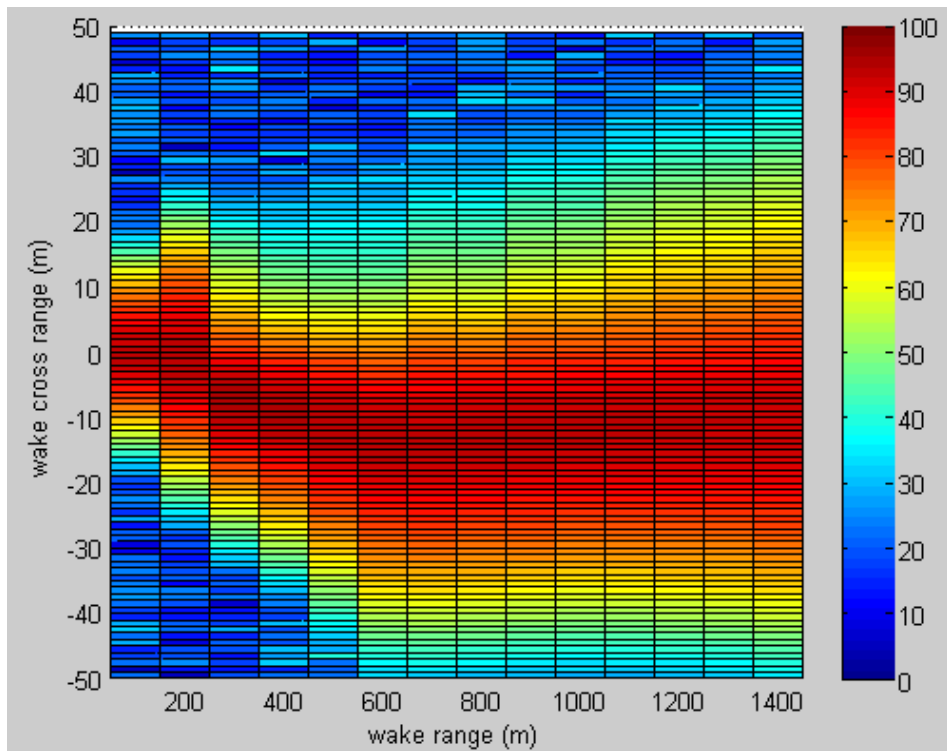


Figure 4.6 Receive level profile with 30 kHz source.

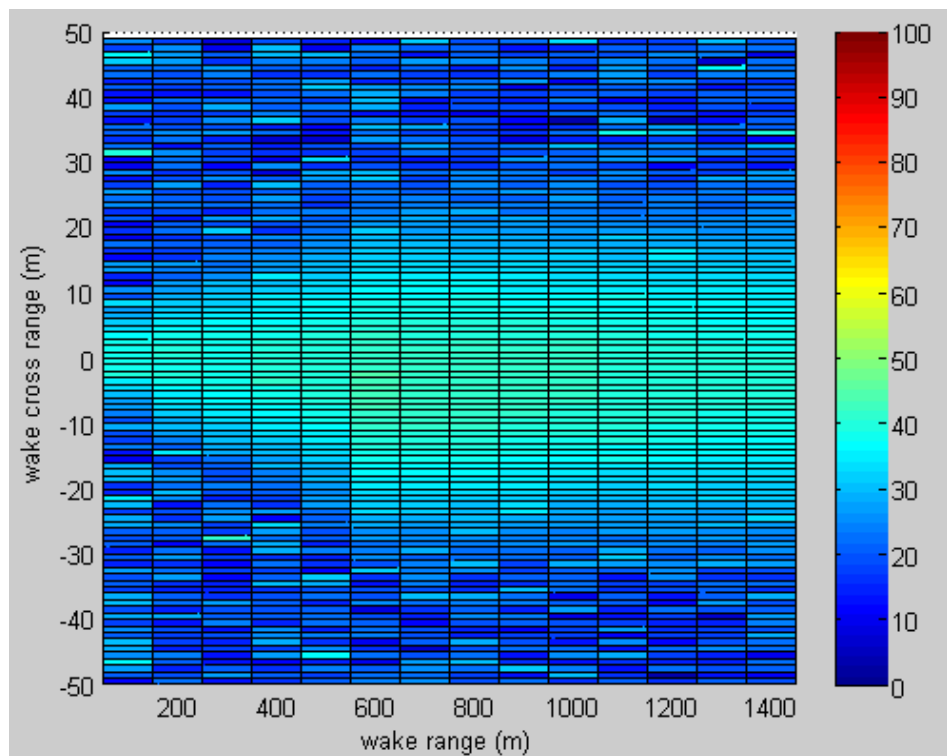


Figure 4.7 Receive level profile with 200 kHz source.

When there is enough amount of resonant bubbles inside the wake, the target strength of the wake is high enough for detection. Also the transmission loss caused by the bubbles is high, decreasing the receive level of the wake cells behind.

For 1 kHz and 200 kHz source frequencies which are out of the resonant frequency range for the wake model used, the receive level considerably decreases. As seen from Figures 4.4 and 4.7, also the receive level profile becomes more symmetric with respect to the axis of wake range. Frequency dependency of wake echo level is another feature that could be exploited for wake detection.

Using a number of sources and receivers at different locations and with different frequency bands, the above features could be used to support the detection of ship wakes. After detection has been ensured, tracking can be maintained by tracing the pattern changes in the receive profiles obtained by source receiver pairs. A database which shows the relation between the receive level profiles and the wake parameters, source frequency, source range, aspect, and wake range would be helpful for matching the observed receive level profiles with a specific situation. Also a database which shows the relation between the ship parameters, the wake parameters and the receive level profiles could be used for classification.

4.3 Tracking with Particle Filter

As mentioned in the previous chapter, after detection has been ensured, tracking of the ship wake, hence tracking of the ship, can be maintained by tracing the pattern changes in the receive profiles obtained by source receiver pairs and matching with a database. Another alternative for tracking the target ship is to use Bayesian filtering methods.

In [66], a detection and tracking algorithm is described to detect and track a ship. The strong noise created by propeller cavitation is used to estimate the bearing of the starting point of the wake. Then a linear feature corresponding to the wake is determined using a high frequency active sonar. This increases the confidence of target detection and also provides initial estimates of target position and velocity. Kalman filter is used for tracking the starting point of the wake, hence the target ship.

In this section, particle filter method [219-222] will be used for tracking based on wake echo measurements. Particle filter method is used instead of Kalman filter method, since wake echo measurement is a nonlinear function of target position and the measurement noise is non-Gaussian. Compared with the method in [66], it is not necessary for the target, namely the start point of the wake, to be inside the search range.

For the first simulation case, the area to be searched is defined as an x-y plane with x-axis extending from 0 m to 4000 m, and y-axis extending from 0 m to 1000 m. Along x-axis at $y = 0$ m, beginning from 1500 m until 2500 m, at each 100 m, source-receiver pairs are located at 3 m depth. The search area is insonified with

a source frequency of 10 kHz. Simulation results are given for a straight going target and one making a triangular path. It is assumed that the wake characteristics of the target are known and determined by the wake model indicated in Section 3.2.

1) The algorithm used for tracking is as follows (Figure 4.8):

The existence of wake inside the search range is determined.

Each 10 kHz source beam is made parallel to the y-axis and insonify 10 m^3 cells of the search range along the beam. For each source, the echo levels from the 10 m^3 cells are summed. If the summation is above a predetermined threshold for consecutive sources, then it is likely that wake exists at that interval. The existence of wake can be confirmed further by using the methods described in Section 4.2.

2) The orientation of the wake is found.

For the wake model used, with 10 kHz source frequency, the echo level will be maximum at the axis of the wake along the wake range. For each source beam insonifying the wake, the maximum echo level and its corresponding location is determined. The location of the maximum echo levels of consecutive parts of the wake gives the orientation of the axis of the wake, hence the orientation of the wake. The direction of the target can be found by observing the evolution of the wake pattern and by observing the echo level pattern of consecutive parts of the wake.

3) Particle filter method is used for tracking.

After the location and the orientation of the wake are determined, the position of the target can be estimated using wake echo level measurements. The relation between the echo levels and the position of the target can be formulated using the wake model. The tracking of target position is made using particle filter method which is explained below.

3.1) Particle sets and particle weights for x and y coordinates of the target are initialized.

The state vector to be estimated is composed of x and y coordinates of the target. Each of the probability density functions for x and y coordinates of the target are represented by 100 particles which are samples of x-axis and y-axis with assigned weights representing the probability density. Since x and y coordinates of the target are uncoupled in the dynamics model of the target given by Eq. (4.4), separate particle sets are used for x and y coordinates. Initially x-axis and y-axis are sampled uniformly and the initial weight $w_{x,0}^i$ of each x-axis sample and the initial weight $w_{y,0}^i$ of each y-axis sample are assigned as 1/100 giving equal probability to the samples, where i is the sample number.

3.2) Measurements of the echo level are done.

The sources are arranged to send transmit beams orthogonally to the wake axis. For each receiver, the echo levels from the 10 m^3 cells are summed. The first

receiver that exceeds the predetermined summation threshold is identified. Propagation loss differences for different portions of the wake are taken into account when making the related calculations. The x and y coordinates corresponding to the maximum echo level received by the chosen receiver and echo level summation of cells in an interval of 20 m of the maximum echo level are recorded.

The measurement function can be represented by

$$M = f(x, y, z) + N \quad (4.1)$$

where M stands for the measurement result, (x, y, z) is the measurement point, and N is the measurement noise.

The measurement function in Eq. (4.1) is a complex nonlinear function that depends on environment parameters like sea state and currents, ship parameters like maneuvering, and measurement parameters like source frequency. As echo measurement noise, besides a background Gaussian noise with a mean of 20 dB and a standard deviation of 6 dB, a uniform random value between [-15,15] dB is added to receive level of each 10 m^3 cells.

For the wake model used, the wake is divided into seven portions along its range. Also, seven intervals for the wake receive level summation is determined. The intervals are numbered from one to seven starting with the interval having the highest receive level summations. For each wake portion, probabilities $p(M|r)$ are assigned for insonifying the portion of the wake at wake range r and receiving echo level summation in those seven intervals.

The difference x_d between the x -coordinate of the target x , and the x -coordinate of the measurement point x_m is given by $r \cos \theta$ and the difference y_d between the y -coordinate of the target y , and the y -coordinate of the measurement point y_m is given by $r \sin \theta$, where θ is the angle of orientation of the wake.

The assigned probabilities which form the perception model are shown in Table 4.1 and are found from 100 simulations. The probabilities $p(M|x_d)$ and $p(M|y_d)$ are the same as the corresponding $p(M|r)$ value.

Table 4.1 Probability $p(M | r)$ forming the perception model

M, r (m)	0- 100	100- 200	200- 300	300- 400	400- 500	500- 1000	1000- 1500
> 3850	0.13	0.48	0.02	0	0	0	0
3750-3850	0.71	0.48	0.51	0.05	0	0	0
3700-3750	0.11	0.01	0.30	0.22	0.02	0.01	0
3650-3700	0.03	0.02	0.12	0.47	0.21	0.20	0
3600-3650	0.02	0.01	0.02	0.19	0.44	0.43	0
3500-3600	0	0	0.03	0.07	0.30	0.35	0.37
< 3500	0	0	0	0	0.03	0.01	0.63

3.3) Particle weights are updated according to the measurement data.

The weights of the particles for x and y coordinates are updated as

$$w_{x,t}^i = w_{x,t-1}^i p(M | x_d) \quad (4.2)$$

$$w_{y,t}^i = w_{y,t-1}^i p(M | y_d) \quad (4.3)$$

using the measurement data, namely the echo level summation received by the receiver chosen and x and y coordinates corresponding to the maximum echo level measured by this receiver. Then, the calculated particle weights are normalized such that the sum of particle weights is equal to one for each axis.

3.4) Resampling of the particle sets are done.

After the weights of the particles are updated, resampling of the particle sets are done, where the probability of taking sample i is w_i^i . By resampling, multiple copies of particles with large weights are created, whereas the particles with small

weights are eliminated. Again the weight w_t^i of each sample is assigned equally as $1/100$. The densities of the particles for x and y axis reflect the probability density functions for x and y coordinates of the target.

3.5) Prediction, update, and resampling steps are applied in turn for each insonification.

The search area is insonified with a period T of 12 s. At each insonification, the location and the orientation of the wake are determined. For each insonification; prediction, update, and resampling steps are applied in turn.

In prediction step, the position of the target, namely the particles x_t^i and y_t^i are estimated using the dynamic model of the target and the previous values of the particles x_{t-1}^i and y_{t-1}^i .

The dynamics of the target is given by

$$X_t^i = A.X_{t-1}^i + Bu + R \quad (4.4)$$

where the state vector is defined as

$$X_t^i = \begin{bmatrix} x_t^i \\ y_t^i \end{bmatrix}, \quad (4.5)$$

the system matrix A is

$$A = \begin{bmatrix} 1 & 0 \\ 0 & 1 \end{bmatrix}, \quad (4.6)$$

B is

$$B = \begin{bmatrix} -T \cdot \cos \theta_{t-1} \\ T \cdot \sin \theta_{t-1} \end{bmatrix}, \quad (4.7)$$

where θ is the angle giving the orientation of the wake, u is the target speed which is assumed to be known and equal to 7.5 m/s and R is the process noise. Since matrix B depends on the orientation measurement, also the corresponding noise can be taken into account by R . For the simulations, a Gaussian process noise with zero mean and 40 m standard deviation in the ship movement direction is used. For the intervals where the ship moves along the x direction, also a Gaussian noise with zero mean and 10 m standard deviation is added to the y direction for the filter process noise.

The update and resampling steps are done as explained for the first measurement. The estimated position of the target is found by taking the average of the particles x_t^i and y_t^i after each resampling step.

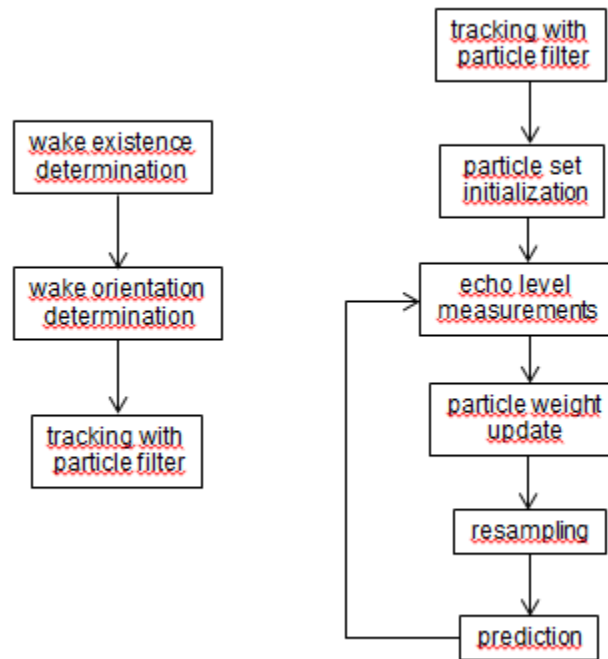


Figure 4.8 Tracking algorithm.

The first simulation is done by a straight going target along the x-axis. The initial position of the target is (1650 m, 500 m). In Figure 4.9, the x and y coordinates of the real position of the target ship, and the estimation of them are shown for an example run.

For this simulation, in addition to the Gaussian process noise with zero mean and 40 m standard deviation in the ship movement direction, also a Gaussian noise with zero mean and 10 m standard deviation is added to the y direction for the process noise.

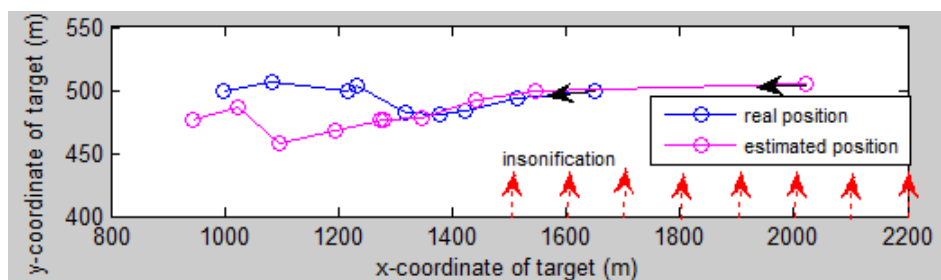


Figure 4.9 Real and estimated coordinates of the target.

The RMSE value for the estimated values the location of the target ship are given in Figure 4.10 using 5 runs.

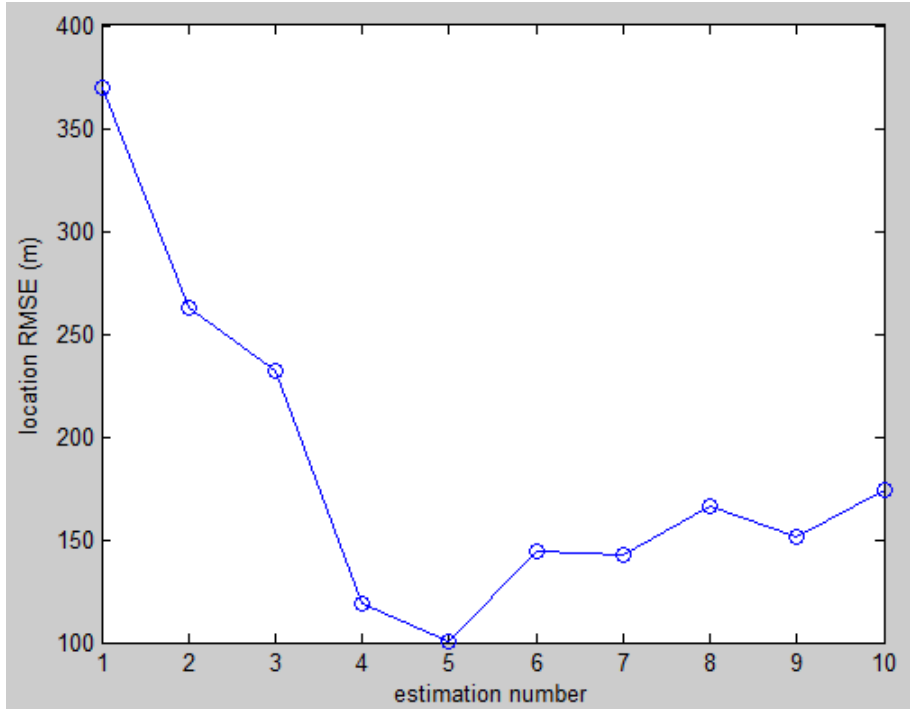


Figure 4.10 RMSE value for the target ship location estimates.

As the ship moves, it gets out of the range of source receiver pairs. The wake orientation measurement is made using the wake far behind the ship, hence estimation error might increase after the ship gets out of range.

The second simulation is done by a target which goes with 45° in decreasing x and increasing y direction for 3 periods, then goes straight in decreasing x direction for 3 periods, and then goes with 45° in decreasing x and decreasing y direction for 4 periods. The initial position of the target is (2150 m, 500 m).

In Figure 4.11, the x and y coordinates of the real position of the target ship, and the estimation of them are shown for an example run. Also, the real and estimated x-coordinate values of the target ship and the real and estimated y-coordinate values of it are given in Figure 4.12 and Figure 4.13 respectively.

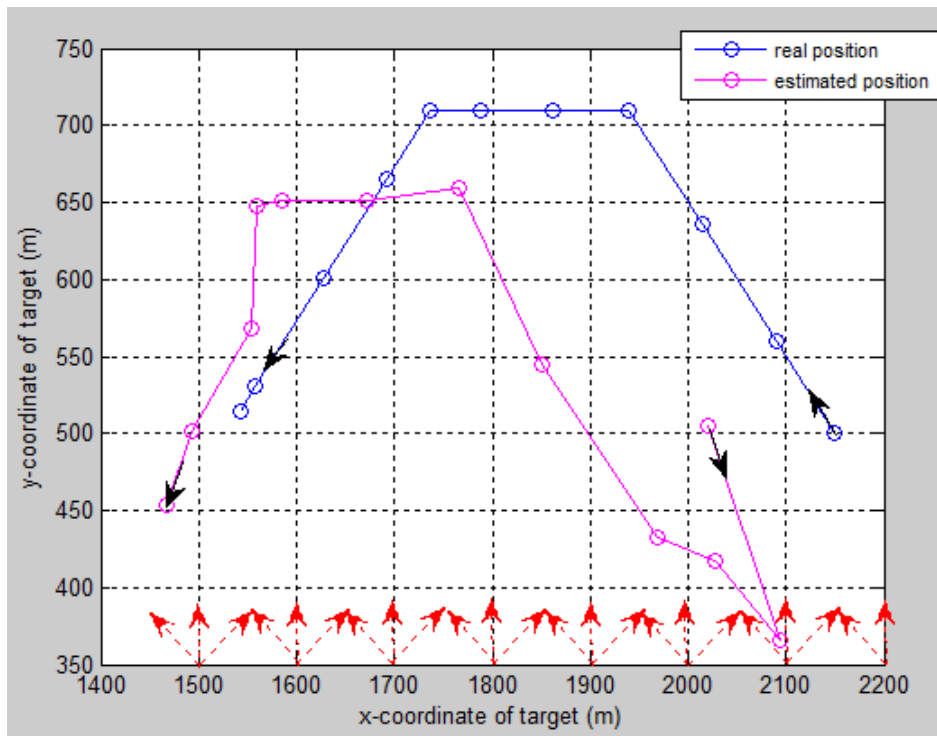


Figure 4.11 Real and estimated coordinates of the target.

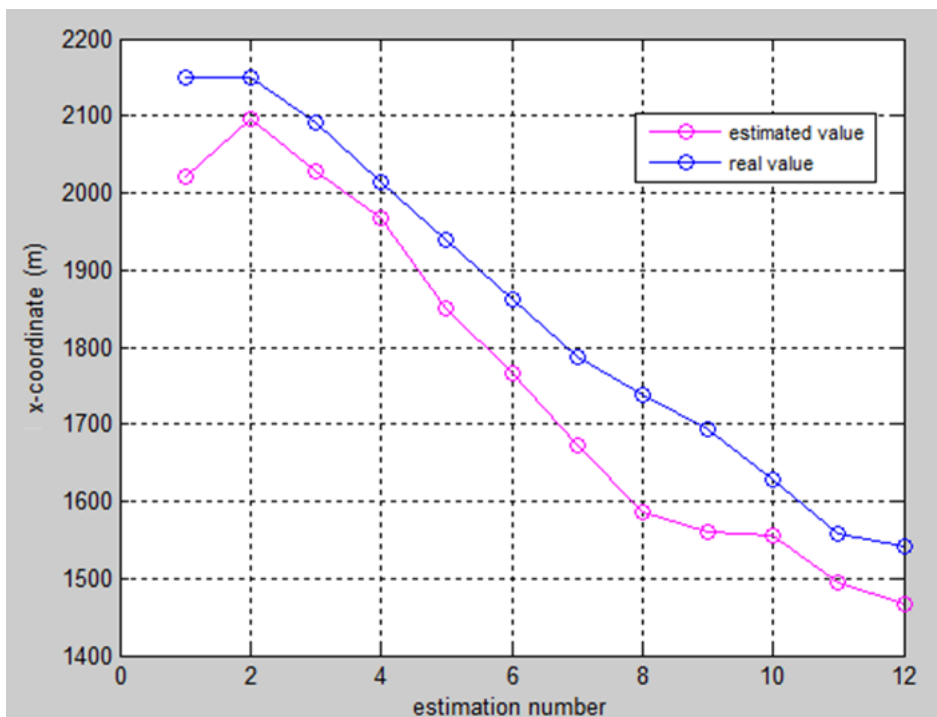


Figure 4.12 Real and estimated x-coordinate values of the target.

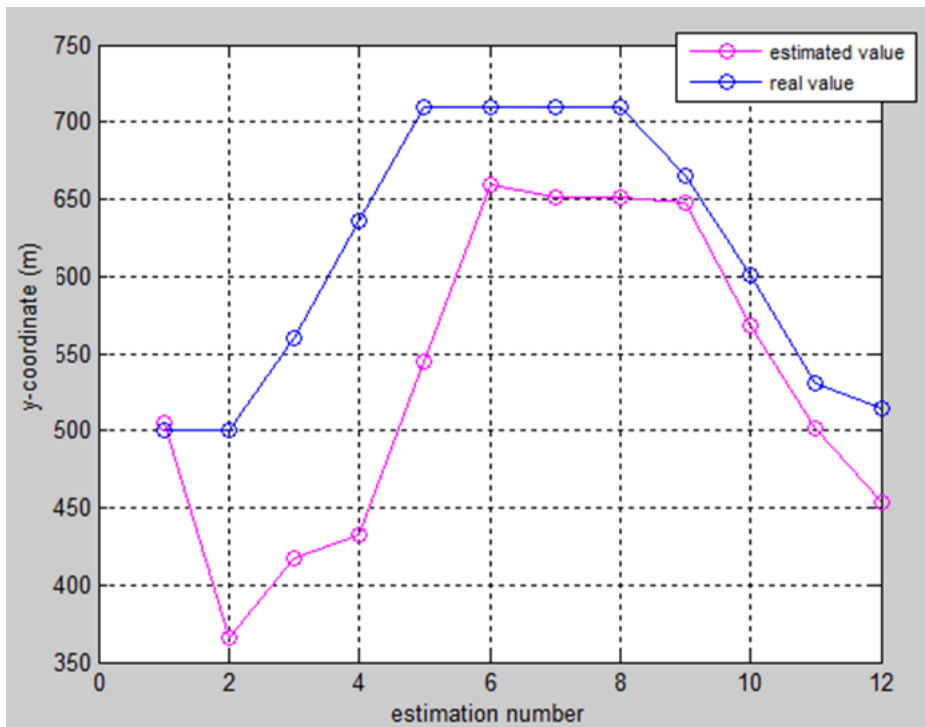


Figure 4.13 Real and estimated y-coordinate values of the target.

For the second simulation case, the area to be searched is defined as an x-y plane with x-axis extending from 0 m to 4000 m, and y-axis extending from 0 m to 2000 m. An underwater vehicle with sensors on each side tracks the ship using the echo measurements. The underwater vehicle is thrown from another ship towards the area of the target ship and travels with a speed of 15 m/s at 3 m depth. The ship wake is insonified with a frequency of 10 kHz.

Simulation results are given for a straight going target and for a target following a triangular path; first along decreasing x direction, then along increasing x direction. Again it is assumed that the wake characteristics of the target are known and determined by the wake model indicated in Section 3.2.

A similar algorithm is followed as in the first simulation case:

- 1) The existence of wake inside the search range is confirmed.

If the echo level summation is above a predetermined threshold for consecutive beams, then it is likely that wake exists at that interval.

- 2) The orientation of the wake is found.

The orientation of the wake is determined in a similar way as in the first case. This time, two beams of the source are used to determine the location of the maximum echo levels of consecutive parts of the wake.

3) Particle filter method is used for tracking.

3.1) Particle sets and particle weights for x and y coordinates of the target are initialized.

3.2) Measurements of the echo level are done.

3.3) Particle weights are updated according to the measurement data.

3.4) Resampling of the particle sets are done.

3.5) The orientation and location of the underwater vehicle for the next insonification are calculated.

The estimated position of the target is found by taking the average of the particles x_t^i and y_t^i . Using the estimate of the target location, the orientation of the underwater vehicle and the location of it for the next insonification are calculated. The orientation of the underwater vehicle is calculated to be directly towards the estimated next position of the target. It is assumed that the vehicle changes its orientation instantly.

3.6) Prediction, update, and resampling steps are applied in turn for each insonification.

The search area is insonified with a period T of 30 s. For each insonification; prediction, update and resampling steps are applied in turn. Using the estimate of the target location, the orientation of the underwater vehicle and the location of it for the next insonification are calculated.

The first simulation is done by a straight going target along the x-axis. In Figure 4.14, the x and y coordinates of the target ship and the underwater vehicle are shown for an example run. The initial position of the target is (1700 m, 1500 m) and the initial position of the underwater vehicle is (2300 m, 0 m).

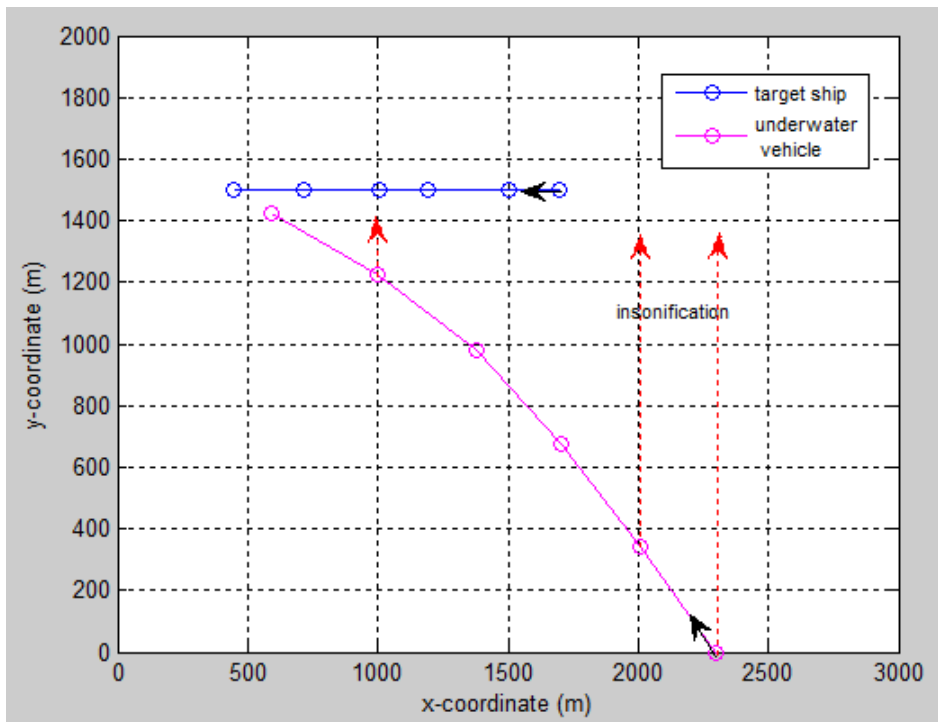


Figure 4.14 Coordinates of the target ship and the underwater vehicle.

The RMSE value for the estimated values of the x-coordinate, y-coordinate, and the location of the target ship are given in Figure 4.15, Figure 4.16, and Figure 4.17 respectively using 5 runs.

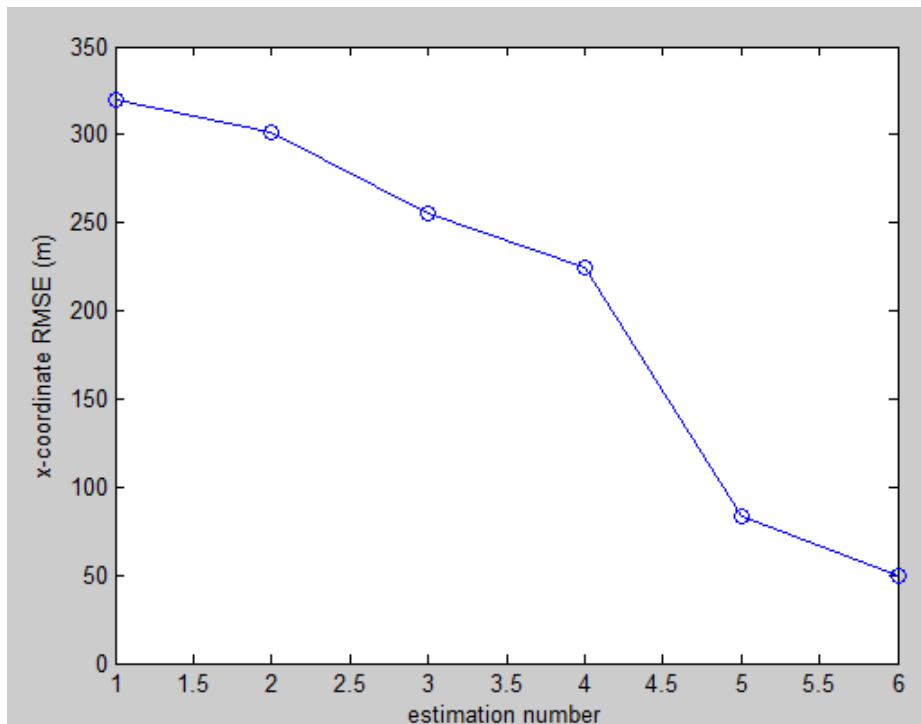


Figure 4.15 RMSE value for the target ship x-coordinate estimates.

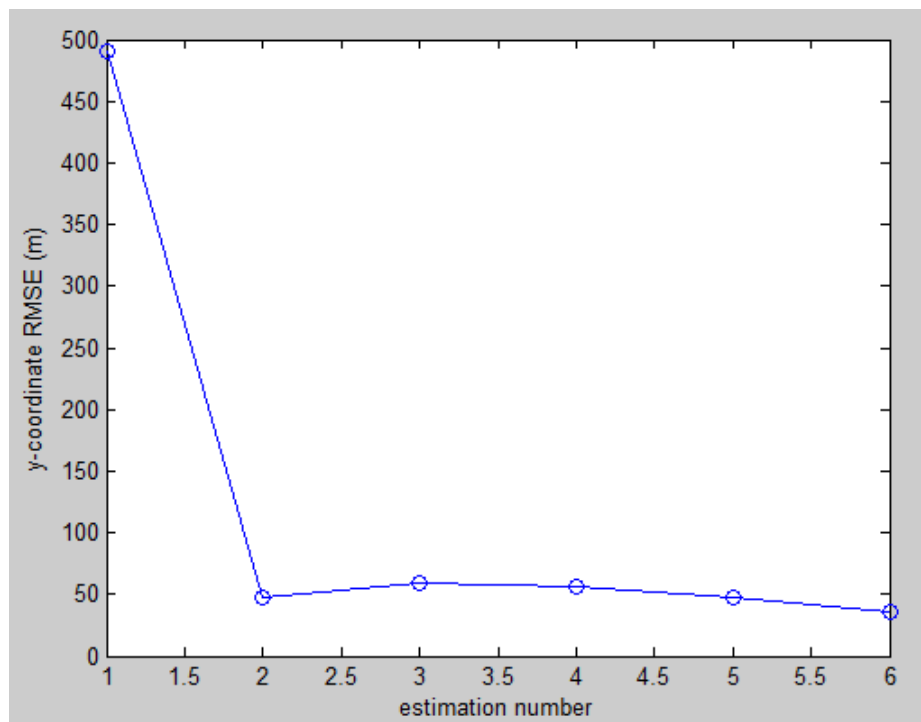


Figure 4.16 RMSE value for the target ship y-coordinate estimates.

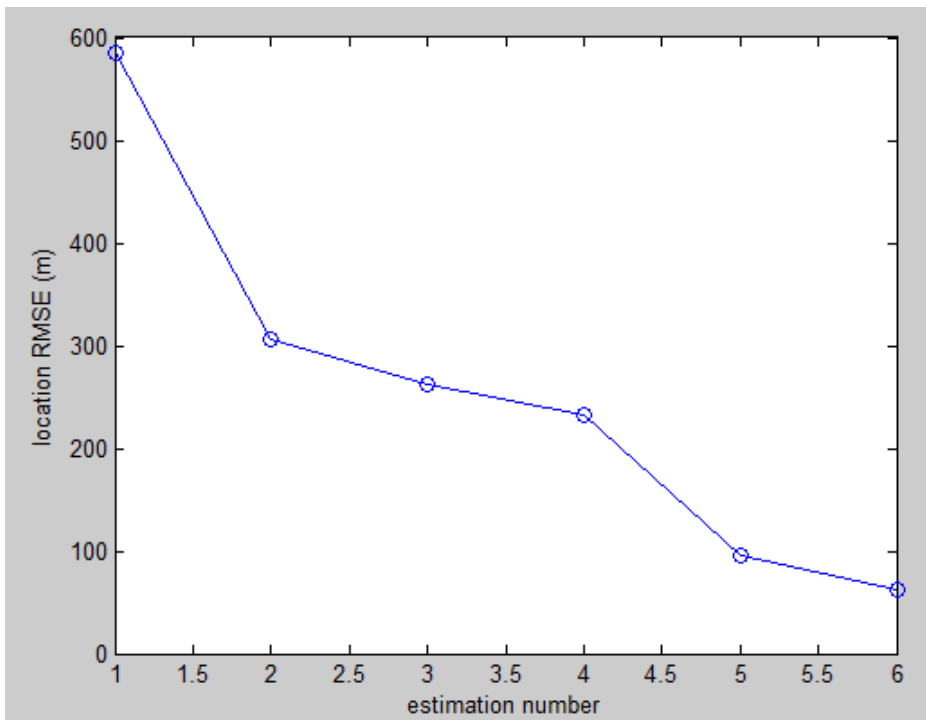


Figure 4.17 RMSE value for the target ship location estimates.

For this configuration, the underwater vehicle tracks the target ship successfully using the particle filter method.

The second simulation is done by a target following a triangular path; first along decreasing x direction, then along increasing x direction. In Figure 4.18, the x and y coordinates of the target ship and the underwater vehicle are shown for an example run. The initial position of the target is (2000 m, 800 m) and the initial position of the underwater vehicle is (2400 m, 0 m).

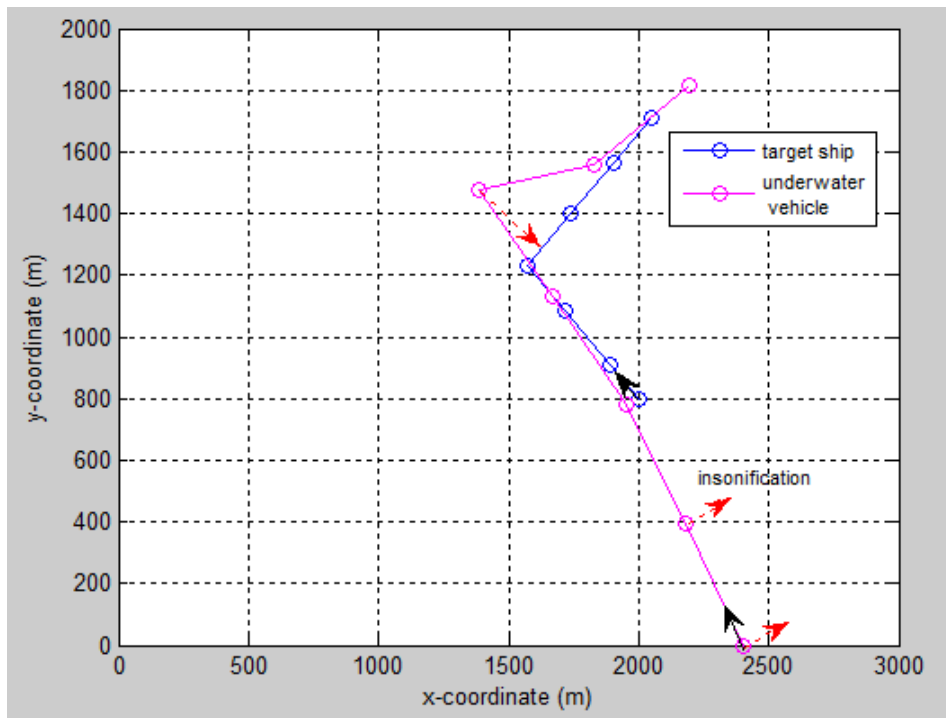


Figure 4.18 Coordinates of the target ship and the underwater vehicle.

The RMSE value for the estimated values of the x-coordinate, y-coordinate, and the location of the target ship are given in Figure 4.19, Figure 4.20, and Figure 4.21 respectively using five runs.

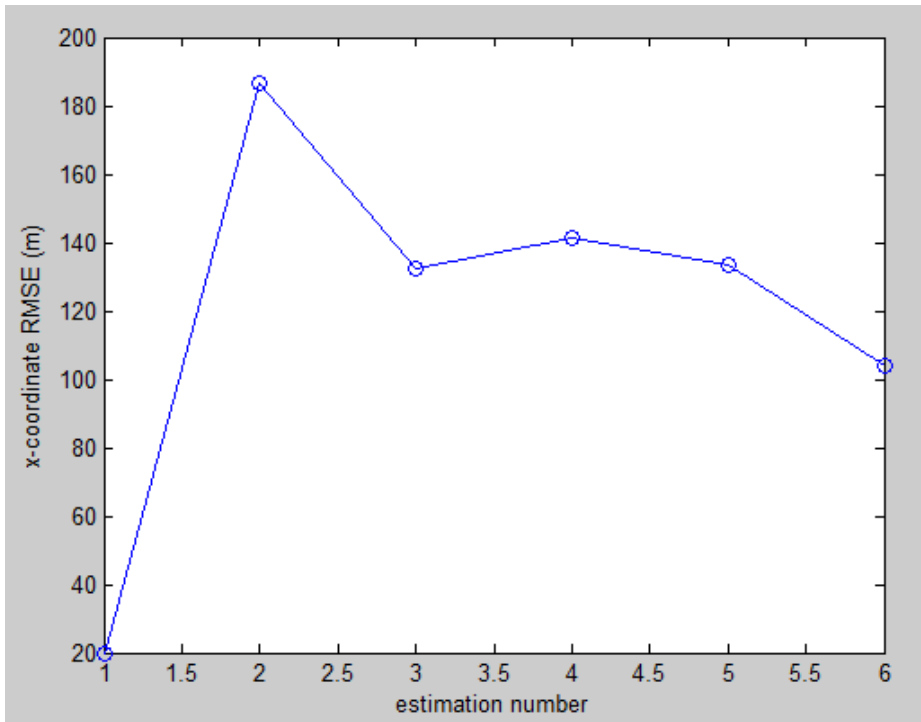


Figure 4.19 RMSE value for the target ship x-coordinate estimates.

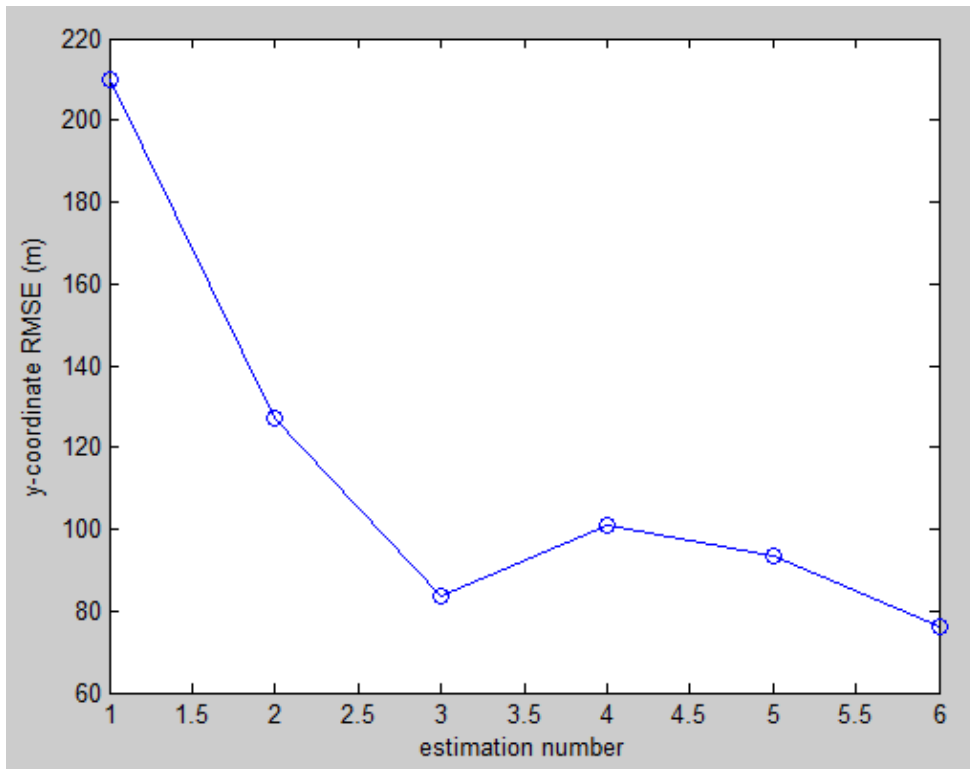


Figure 4.20 RMSE value for the target ship y-coordinate estimates.

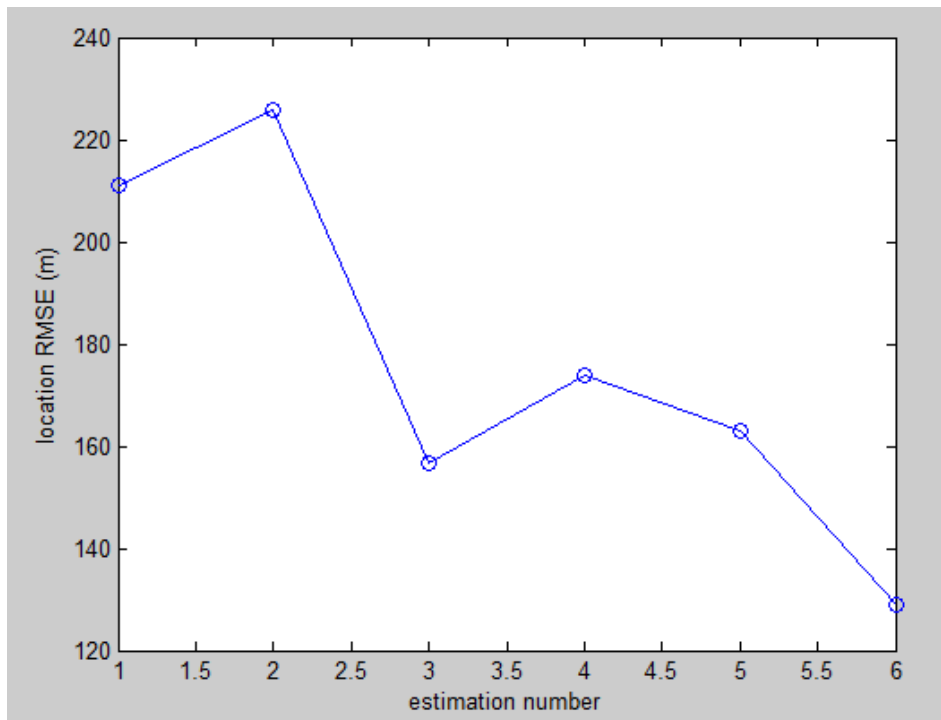


Figure 4.21 RMSE value for the target ship location estimates.

For this configuration, again the underwater vehicle tracks the target ship successfully using the particle filter method.

With the wake and noise models used, the implemented particle filter algorithm gives successful results for tracking ships using wake echo measurements. The results depend on the simulation configuration and the target path.

CHAPTER 5

CONCLUSIONS

Research and simulations have been carried out for detection and tracking of ship wakes. A simulation environment is developed in Matlab and results of related numerical experiments are given.

The wake model described in [102] is taken as the basis for the wake profiles used in this thesis. Since the mean bubble density profile of the wake model in [102] depends on data found in the literature, it is supposed that the wake model will give realistic and sufficient results for the studies related to this thesis.

The wake model described in [102] is simulated with some modifications. Mainly the bubble size distribution of the wake model is changed, taking into account that small sized bubbles last for a longer time than bigger sized bubbles.

Receive level profiles when insonifying ship wake are obtained using this wake model. Some features of the ship wake echo level pattern that could be exploited for detection and tracking are outlined.

For the wake model used, it has been observed that changing the source frequency, both the magnitude and the symmetry of the receive level profile of the wake with respect to the wake range axis changes.

Particle filter method has been implemented with Matlab for target tracking using wake echo measurements. Particle filter is used instead of Kalman filter method, since wake echo measurement is a nonlinear function of target position.

With the wake and noise models used, it has been observed that the implemented particle filter algorithm gives successful results for tracking ships using wake echo measurements. The results depend on the simulation configuration and the target path.

Ship wake structure used in this thesis is based on the knowledge found in the literature. A complete model of the ship wake structure that includes the initial bubble distribution and the evolution of the bubble distribution in relation with the ship and ambient parameters is needed to obtain more realistic results for the scattering characteristics of ship wakes. Also, the effects of maneuvering should be taken into account. For a complete model like this, not only theoretical and numerical studies but also ocean experiments would be necessary.

Scattering characteristics of the bubble clouds in ship wakes are modeled based on linear harmonic oscillator model of bubbles and multiple scattering theory. As a future work, nonlinear behavior of the bubbles could be taken into account in modeling scattering characteristics of the bubble clouds in ship wakes.

Forward studies could be done using advanced sonar and environment models which would give more precise results. Signal processing methods should be developed for environment with intensive noise and clutter.

Also, for a thorough understanding of the processes related to acoustic detection and tracking of ship wakes, laboratory studies and ocean experiments should be carried out in addition to numerical experiments.

REFERENCES

- [1] T. C. Weber. "Acoustic Propagation Through Bubble Clouds". Ph.D. Thesis, The Pennsylvania State University, May 2006.
- [2] T. G. Leighton. "The Acoustic Bubble". Academic Press, 1997.
- [3] S. Vagle, D. M. Farmer. "The Measurement of Bubble-Size Distributions by Acoustical Backscatter". *Journal of Atmospheric and Oceanic Technology*, vol. 9, October 1992.
- [4] S. Vagle, D. M. Farmer. "A Comparison of Four Methods for Bubble Size and Void Fraction Measurements". *IEEE Journal of Oceanic Engineering*, vol. 23, no. 3, July 1998.
- [5] J. C. Novarini, R. S. Keiffer, and G. V. Norton. "A Model for Variations in the Range and Depth Dependence of the Sound Speed and Attenuation Induced by Bubble Clouds Under Wind Driven Sea Surfaces". *IEEE Journal of Oceanic Engineering*, vol. 23, no. 4, October 1998.
- [6] A. Sutin, A. Benilov, H.-S. Roh, Y.I. Nah. "Acoustic Measurements of Bubbles in the Wake of Ship Model in Tank". *Proceedings of the Ninth European Conference on Underwater Acoustics, ECUA 2008*.
- [7] D. L. Bradley, R. L. Culver, X. Di, L. Bjørnø. "Acoustic Qualities of Ship Wakes". *Acta Acustica United with Acustica*, vol. 88, 2002.
- [8] A. Prosperetti, N. Q. Lu, H. S. Kim. "Active and Passive Acoustic Behavior of Bubble Clouds at the Ocean's Surface". *The Journal of the Acoustical Society of America*, vol. 93, June 1993.
- [9] J. W. Caruthers, P. A. Elmore, J.C. Novarini, R. R. Goodman. "An Iterative Approach for Approximating Bubble Distributions from Attenuation Measurements". *The Journal of the Acoustical Society of America*, vol. 106, July 1999.
- [10] S. Stanic, J. W. Caruthers, R. R. Goodman, E. Kennedy, R. A. Brown. "Attenuation Measurements Across Surface-Ship Wakes and Computed Bubble Distributions and Void Fractions". *IEEE Journal of Oceanic Engineering*, vol. 34, no. 1, January 2009
- [11] T. G. Leighton, A. D. Phelps, D.G. Ramble. "Bubble Detection Using Low Amplitude Multiple Acoustic Techniques". *Proceedings of the Third European Conference on Underwater Acoustics, ECUA 1996*.
- [12] P. Schippers. "Coherent Target Scattering in the Active Sonar Performance Model ALMOST/REACT". *Proceedings of the Seventh European Conference on Underwater Acoustics, ECUA 2004*.
- [13] T. Leighton, D. Finfer, P. White. "Experimental Evidence for Enhanced Target Detection by Sonar in Bubbly Water". *Hydroacoustics*, vol. 11, 2008.

- [14] P.R. White, T.G. Leighton, G.T. Yim. "Exploitation of Higher Order Statistics to Compute Bubble Cloud Densities; Evading Olber's Paradox". Proceedings of the Seventh European Conference on Underwater Acoustics, ECUA 2004.
- [15] M. Trevorrow. "High Frequency Acoustic Scattering and Absorption Effects Within Ship Wakes". Report: DRDC-ATLANTIC-SL-2005-125, DRDC, August 2005.
- [16] R. Lee Culver, M. F. Trujillo. "Measuring and Modeling Bubbles in Ship Wakes, and Their Effect on Acoustic Propagation". Proceedings of the Second International Conference on Underwater Acoustic Measurements: Technologies and Results, 2007.
- [17] P. Schippers. "Modelling Analysis of Echo Signature and Target Strength of a Realistically Modelled Ship Wake for a Generic Forward Looking Active Sonar". Proceedings of the Third International Conference on Underwater Acoustic Measurements: Technologies and Results, 2009.
- [18] T. G. Leighton. "Nonlinear Bubble Dynamics And The Effects On Propagation Through Near-Surface Bubble Layers". High-Frequency Ocean Acoustics, M.B. Porter, M. Siderius, W. A. Kuperman, Eds., AIP Conference Proceedings, 2004.
- [19] T.G. Leighton, H.A. Dumbrell, G.J. Heald, P.R. White. "The Possibility and Exploitation of Nonlinear Effects in the Near Surface Oceanic Bubble Layer". Proceedings of the Seventh European Conference on Underwater Acoustics, ECUA 2004.
- [20] T. G. Leighton, S. D. Meers, P. R. White. "Propagation Through Nonlinear Time-dependent Bubble Clouds and the Estimation of Bubble Population from Measured Acoustic Characteristics". Proceedings of the Royal Society, vol. 460, 2004.
- [21] T. C. Weber. "Observations of Clustering Inside Oceanic Bubble Clouds and the Effect on Short-Range Acoustic Propagation". The Journal of the Acoustical Society of America, vol. 124, November 2008.
- [22] T.G. Leighton, A.D. Phelps, D.G. Ramble, D.A. Sharpe. "Comparison of the Abilities of Eight Acoustic Techniques to Detect and Size a Single Bubble". Ultrasonics, vol. 34, Elsevier, 1996.
- [23] V. Duro, D. R. Rajaona, D. Décultot, G. Maze. "Experimental Study of Sound Propagation Through Bubbly Water; Comparison with Optical Measurements". IEEE Journal of Oceanic Engineering, vol. 36, no. 1, January 2011.
- [24] K. P. Yeo, E. Taylor, S. H. Ong. "Modeling Backscatter of Marine Mammal Biomimetic Sonar Signals from Bubble Clouds". IEEE Conference Proceedings of Oceans 2010.
- [25] A. Ishimaru. "Wave Propagation and Scattering in Random Media". IEEE Press, 1997.
- [26] "Physics of Sound in the Sea". Department of the Navy Headquarters Naval Material Command, Washington, D.C., 1969.

- [27] A. D. Waite. "Sonar for Practising Engineers". John Wiley and Sons, 2002.
- [28] R. J. Urick. "Principles of Underwater Sound". Peninsula Publishing, 1983.
- [29] S. Stanic, E. Kennedy, B. Brown, D. Malley, R. Goodman, J. Caruthers. "Broadband Acoustic Transmission Measurements in Surface Ship Wakes". IEEE Conference Proceedings of Oceans 2007.
- [30] L. L. Foldy. "The Multiple Scattering of Waves". Physical Review, vol. 67, 1945.
- [31] K. Commander, E. Moritz. "Off-resonance Contributions to Acoustical Bubble Spectra". The Journal of the Acoustical Society of America, vol. 85, June 1989.
- [32] J. C. Cochran. "Elements of Sonar Transducer Design". ATI's Course Book, 2011.
- [33] P. C. Etter. "Underwater Acoustic Modeling and Simulation". Spon Press, 2003.
- [34] E. J. Terrill, W. K. Melville. "A Broadband Acoustic Technique for Measuring Bubble Size Distributions: Laboratory and Shallow Water Measurements". Journal of Atmospheric and Oceanic Technology, Vol. 17, 2000.
- [35] J. W. Caruthers, S. J. Stanic, P. A. Elmore, R. R. Goodman. "Acoustic Attenuation in Very Shallow Water Due to the Presence of Bubbles in Rip Currents". The Journal of the Acoustical Society of America, vol. 106, August 1999.
- [36] B. K. Choi, S. W. Yoon. "Acoustic Bubble Counting Technique Using Sound Speed Extracted from Sound Attenuation". IEEE Journal of Oceanic Engineering, vol. 26, no. 1, January 2001.
- [37] A. D. Phelps, T. G. Leighton. "Acoustic Bubble Sizing Using Two Frequency Excitation Techniques". Proceedings of the Second European Conference on Underwater Acoustics, ECUA 1994.
- [38] Z. Ye, L. Ding. "Acoustic Dispersion and Attenuation Relations in Bubbly Mixture". The Journal of the Acoustical Society of America, vol. 98, September 1995.
- [39] S. Finette, D. Tielbuerger. "Acoustic Intensity Fluctuations in a Stochastic Shallow Water Waveguide Caused by Scattering From Near Surface Bubble Clouds". Proceedings of the Third European Conference on Underwater Acoustics, ECUA 1996.
- [40] S. Vagle, H. Burch. "Acoustic Measurements of the Sound-Speed Profile in the Bubbly Wake Formed by a Small Motor Boat". The Journal of the Acoustical Society of America, vol. 117, January 2005.
- [41] T. C. Weber, A. P. Lyons, D. L. Bradley. "Acoustic Propagation Through Clustered Bubble Clouds". IEEE Journal of Oceanic Engineering, vol. 32, no. 2, April 2007.

- [42] S. Stanic, T. Ruppel, R. Goodman. "Acoustic Propagation Through Surface Ship Wakes". NRL Review, 2006.
- [43] G. C. Gaunard, H. Huang. "Acoustic Scattering by an Air Bubble Near the Sea Surface". IEEE Journal of Oceanic Engineering, vol. 20, no. 4, April 1995.
- [44] V. Duro, D. Rajaona, D. Decultot, G. Maze. "Acoustical and Optical Measurements on a Mixture of Air Microbubbles in Water". Proceedings of the Ninth European Conference on Underwater Acoustics, ECUA 2008.
- [45] A. I. Best, M. D. J. Tuffin, J. K. Dix, J. M. Bull. "Acoustical Behaviour of Gas Bearing Marine Sediments". Proceedings of the Seventh European Conference on Underwater Acoustics, ECUA 2004.
- [46] G. A. Postnov. "Acoustical Field of Pointlike Source in Water Positioned in the Centre of Air Bubble Spherical Cloud". Proceedings of the Fifth European Conference on Underwater Acoustics, ECUA 2000.
- [47] G. B. Deane, M. D. Stokes. "Air Entrainment Processes and Bubble Size Distributions in the Surf Zone". Journal of Physical Oceanography, vol. 29, July 1999.
- [48] A. Dragan, Z. Klusek, A. Lisimenka. "Ambient Noise, Bubble Clouds and Wind Speed Relationships". Proceedings of the Tenth European Conference on Underwater Acoustics, ECUA 2010.
- [49] S.A.S. Jones, S. D. Richards, J. R. Martin. "Ambient Noise Measurements for Surf-Zone Characterization". Proceedings of the Fifth European Conference on Underwater Acoustics, ECUA 2000.
- [50] P. R. White, W. B. Collis, T. G. Leighton. "Analysis of Bubble Scattering Data using Higher Order Statistics". Proceedings of the Third European Conference on Underwater Acoustics, ECUA 1996.
- [51] A. Baranowska, Z. Klusek. "Analysis of Nonlinear Generation in Bubble Layer". Proceedings of the Tenth European Conference on Underwater Acoustics, ECUA 2010.
- [52] H. Herwig, B. Nützel. "Attenuation and Scattering by Bubbles and Their Influence on Surface Backscattering Strength". Proceedings of the Second European Conference on Underwater Acoustics, ECUA 1994.
- [53] H. Mizushima, T. Makit, T. Urat, T. Sakamakit, H. Kondot, M. Yanagisawa. "Autonomous Recognition of Bubble Plumes for Navigation of Underwater Robots in Active Shallow Vent Areas". IEEE Conference Proceedings of Oceans 2007.
- [54] K. Sarkar, A. Prosperetti. "Backscattering of Underwater Noise by Bubble Clouds". The Journal of the Acoustical Society of America, vol. 93, June 1993.
- [55] M. B. Stewart, E. W. Miner. "Bubble Dynamics in a Turbulent Ship Wake". NRL Memorandum, November 1987.
- [56] J. Wu. "Bubbles in the Near-Surface Ocean: Their Various Structures". Journal of Physical Oceanography, vol. 24, September 1994.

- [57] R. A. Roy, J. A. Schindall, W. M. Carey, L. A. Crum. "Can Near-Surface Bubble Clouds and Plumes Lead to Anomalous Perturbations in Low-Frequency Sea-Surface Scattering?". Proceedings of the Second European Conference on Underwater Acoustics, ECUA 1994.
- [58] A. D. Phelps, D. G. Ramble, T. G. Leighton. "Characterisation of the Oceanic Bubble Population Using a Combination Frequency Technique". Proceedings of the Third European Conference on Underwater Acoustics, ECUA 1996.
- [59] K. Sarkar, A. Prosperetti. "Coherent and Incoherent Scattering by Oceanic Bubbles". The Journal of the Acoustical Society of America, vol. 96, July 1994.
- [60] Z. Ye. 'Comments on "The Attenuation and Dispersion of Sound in Water Containing Multiply Interacting Air Bubbles"'. The Journal of the Acoustical Society of America, vol. 102, August 1997.
- [61] F. S. Henyey. "Corrections to Foldy's Effective Medium Theory for Propagation in Bubble Clouds and Other Collections of Very Small Scatterers". The Journal of the Acoustical Society of America, vol. 105, April 1999.
- [62] M. V. Trevorrow, B. Vasiliev, S. Vagle. "Directionality and Maneuvering Effects on a Surface Ship Underwater Acoustic Signature". The Journal of the Acoustical Society of America, vol. 124, August 2008.
- [63] T. G. Leighton, D. C. Finfer, G. H. Chua, P. R. White, J. K. Dix. "Clutter Suppression and Classification Using Twin Inverted Pulse Sonar in Ship Wakes". The Journal of the Acoustical Society of America, vol. 130, November 2011.
- [64] T. C. Weber, A. P. Lyons, D. L. Bradley. "Consistency in Statistical Moments as a Test for Bubble Cloud Clustering". The Journal of the Acoustical Society of America, vol. 130, November 2011.
- [65] M. A. Ainslie, T. G. Leighton. "Review of Scattering and Extinction Cross-Sections, Damping Factors, and Resonance Frequencies of a Spherical Gas Bubble". The Journal of the Acoustical Society of America, vol. 130, November 2011.
- [66] K. W. Lo, B. G. Ferguson. "Automatic Detection and Tracking of a Small Surface Watercraft in Shallow Water using a High Frequency Active Sonar". IEEE Transactions on Aerospace and Electronic Systems, vol. 40, October 2004.
- [67] D. E. Huff. "Surface Ship Location Based on Active Sonar Image Data". Literature Survey, The University of Texas at Austin, March 2005.
- [68] A. Smirnov, I. Celik, S. Shi. "LES of Bubble Dynamics in Wake Flows". Computers and Fluids, Elsevier, vol. 34, 2005.
- [69] C. S. Clay, H. Medwin. "Acoustical Oceanography: Principles and Applications". John Wiley and Sons, 1977.
- [70] H. Medwin. "Sounds in the Sea: From Ocean Acoustics to Acoustical Oceanography". Cambridge University Press, 2005.

- [71] H. Vorhoelzer, S. Krueger. "Wake Field Analysis of a Drifting Ship with RANS-CFD-Methods". Numerical Towing Tank Symposium, 2008.
- [72] C. Devin. "Survey of Thermal, Radiation, and Viscous Damping of Pulsating of Air Bubbles in Water". The Journal of the Acoustical Society of America, vol. 31, December 1959.
- [73] J. B. Keller, M. Miksis. "Bubble Oscillations of Large Amplitude". The Journal of the Acoustical Society of America, vol. 68, August 1980.
- [74] A. Prosperetti. "Bubble Phenomena in Sound Fields: Part One". Ultrasonics, March 1984.
- [75] R. E. Caflisch, M. J. Miksis, G. C. Papanicolaou, L. Ting. "Effective Equations for Wave Propagation in Bubbly Liquids". Journal of Fluid Mechanics, vol. 153, 1985.
- [76] T. G. Leighton, P. R. White, H. A. Dumbrell, G. J. Heald. "Nonlinear Propagation in Bubbly Water: Theory and Measurement in the Surf Zone". Proceedings of the International Conference on Underwater Acoustic Measurements: Technologies & Results, 2005.
- [77] N. Gorska, D. Chu. "Echo Interference in Acoustic Backscattering by Densely Aggregated Targets". Proceedings of the Seventh European Conference on Underwater Acoustics, ECUA 2004.
- [78] S. G. Kargl. "Effective Medium Approach to Linear Acoustics in Bubbly Liquids". The Journal of the Acoustical Society of America, vol. 111, January 2002.
- [79] R. C. Gauss, E. I. Thorsos. "Frequency Shift Models for Surface and Fish Backscattering". Proceedings of the Seventh European Conference on Underwater Acoustics, ECUA 2004.
- [80] P. D. Osborne, D. B. Hericks, J. M. Cote. "Full-scale Measurements of High Speed Passenger Ferry Performance and Wake Signature". IEEE Conference Proceedings of Oceans 2007.
- [81] A. Nikolovska, A. Ooi, R. Widjaja, R. Manasseh. "Resonant Scattering from a Chain of Air Bubbles in Water". Proceedings of the Seventh European Conference on Underwater Acoustics, ECUA 2004.
- [82] "Underwater Acoustics and Sonar Systems, Course Notes". University of Birmingham, 2010.
- [83] S. Stergiopoulos. "Advanced Signal Processing Handbook". CRC Press, 2001.
- [84] H. Medwin, C. S. Clay. "Fundamentals of Acoustical Oceanography". Elsevier, 1998.
- [85] H. L. V. Trees. "Detection, Estimation, and Modulation Theory". John Wiley and Sons, 1968.

- [86] D. T. I. Francis, K. G. Foote. "Anatomy of Fish Swimbladder Acoustic Resonances at High Frequencies". Proceedings of the Seventh European Conference on Underwater Acoustics, ECUA 2004.
- [87] P. Schippers. "Coherent Effects of Flow and Pressure Hull of a Generic Submarine on Target Scattering in an Active Sonar Performance Model". Proceedings of the Ninth European Conference on Underwater Acoustics, ECUA 2008.
- [88] D. L. Bradley. "High Frequency Acoustics and Signal Processing for Weapons". The Pennsylvania State University, ARL Report, November 2001.
- [89] A. M. Sutin, S. W. Yoon, E. J. Kim, I. N. Didenkulov. "Nonlinear Acoustic Method for Bubble Density Measurements in Water". The Journal of the Acoustical Society of America, vol. 103, May 1998.
- [90] A. Soloviev, M. Gilman, K. Young, S. Bruschi, S. Lehner. "Sonar Measurements in Ship Wakes Simultaneous with TerraSAR-X Overpasses". IEEE Transactions on Geoscience and Remote Sensing, vol. 48, no. 2 February 2010.
- [91] J. Szczucka. "Sound Scattering from Gas Bubbles in the Sea - Numerical Consideration of Coherence and Interaction Effects". Proceedings of the Second European Conference on Underwater Acoustics, ECUA 1994.
- [92] R. van Vossen, M. A. Ainslie. "The Effect of Wind Generated Bubbles on Sea-Surface Backscattering at 940 Hz". The Journal of the Acoustical Society of America, vol. 130, November 2011.
- [93] G. V. Norton, J. C. Novarini. "Time Domain Modelling of Backscattering from an Aggregate of Bubble Plumes Beneath The Sea Surface Including Attenuation and Dispersion Effects". Proceedings of the Seventh European Conference on Underwater Acoustics, ECUA 2004.
- [94] J. L. Leander. "Wave Front Speed and Group Velocity in Bubbly Fluids". Proceedings of the Fourth European Conference on Underwater Acoustics, ECUA 1998.
- [95] E. Barlow, A. J. Mulholland. "A Fractional Fourier Transform Analysis of a Bubble Excited by an Ultrasonic Chirp". The Journal of the Acoustical Society of America, vol. 130, November 2011.
- [96] V. A. Akulichev, V. A. Bulanov. "Measurements of Bubbles in Sea Water by Nonstationary Sound Scattering". The Journal of the Acoustical Society of America, vol. 130, November 2011.
- [97] G. Welch, G. Bishop. "An Introduction to the Kalman Filter". University of North Carolina at Chapel Hill, July 2006.
- [98] K. A. Johannesson, R. B. Mitson. "Fisheries Acoustics: A Practical Manual for Aquatic Biomass Estimation". Food and Agriculture Organization of the United Nations, 1983.

- [99] C. G. Hempel. "Adaptive Track Detection for Multi-Static Active Sonar Systems". IEEE Conference Proceedings of Oceans 2006.
- [100] G. O. Marmorino, C. L. Trump. "Preliminary Side-Scan ADCP Measurements Across a Ship's Wake". Journal of Atmospheric and Oceanic Technology, vol. 13, April 1996.
- [101] R. L. Culver, T. C. Weber, D. L. Bradley. "The Use of Multi-Beam Sonars to Image Bubbly Ship Wakes". Proceedings of the International Conference on Underwater Acoustic Measurements: Technologies & Results, 2005.
- [102] B. R. Rapids, R. L. Culver. "An Acoustic Ship Wake for Propagation Studies". The Pennsylvania State University, ARL Technical Memorandum, April 2000.
- [103] R. J. P. van Bree, H. Greidanus. "Ship Wake Current Models and Bubble Distributions". TNO Report, July 2012.
- [104] T. C. Gallaudet. "Acoustic Propagation Through Bubble Clouds". Ph.D. Thesis, University of California, 2001.
- [105] A. Skoelv, T. Wahl, S. Eriksen. "Simulation of SAR Imaging of Ship Wakes". Proceedings of IGARSS '88 Symposium, 1988.
- [106] A. Skoelv. "Simulation of SAR Imaging of Ship Wakes, Comparing Different Wind Growth Rate Models". Proceedings of IGARSS '91 Symposium, 1991.
- [107] P. Schippers. "Analysis of Target Strength Variation; Results of a Realistic Wake Echo Structure Model Compared with Side Scan Sonar Pictures". Proceedings of the Second International Conference on Underwater Acoustic Measurements: Technologies and Results, 2007.
- [108] M. V. Trevorrow. "Volumetric Multibeam Sonar Measurements of Fish, Zooplankton, and Turbulence". Proceedings of the International Conference on Underwater Acoustic Measurements: Technologies & Results, 2005.
- [109] I. T. Ruiz, Y. Petillot, Y. de Saint-Pern. "Detection and Tracking of Pipes in Sonar Data". Proceedings of the International Conference on Underwater Acoustic Measurements: Technologies & Results, 2005.
- [110] K. Abe, K. Sadayasu, K. Sawada, K. Ishii, Y. Takao. "Precise Target Strength Measurement of Juvenile Walleye Pollock with Consideration for Morphology of Swimbladder". Proceedings of the International Conference on Underwater Acoustic Measurements: Technologies & Results, 2005.
- [111] A. Milewski, E. Sedek, S. Gawor. "The Method of Amplitude Weighting of Linear Frequency Modulated Chirp Signals for Sonar Application". Proceedings of the Second International Conference on Underwater Acoustic Measurements: Technologies and Results, 2007.
- [112] T. G. Leighton, D.C. Finfer, P. R. White. "Sonar which Penetrates Bubble Clouds". Proceedings of the Second International Conference on Underwater Acoustic Measurements: Technologies and Results, 2007.

- [113] M. A. Ainslie, T. G. Leighton. "The Influence of Radiation Damping on Through Resonance Variation in the Scattering Cross-section of Gas Bubbles". Proceedings of the Second International Conference on Underwater Acoustic Measurements: Technologies and Results, 2007.
- [114] A. Mantouka, T. G. Leighton, V. F. Humphrey. "Enhancement of Nonlinearity and Parametric Sonar Using Bubbles". Proceedings of the Second International Conference on Underwater Acoustic Measurements: Technologies and Results, 2007.
- [115] T. G. Leighton, D.C. Finfer, E. J. Grover, P. R. White. "Spiral Bubble Nets of Humpback Whales: An Acoustic Mechanism". Proceedings of the Second International Conference on Underwater Acoustic Measurements: Technologies and Results, 2007.
- [116] A. R. Amiri-Simkooei, M. Snellen, D. G. Simons. "Using Multi-Beam Echo Sounder Backscatter Data For Sediment Classification in very Shallow Water Environments". Proceedings of the Third International Conference on Underwater Acoustic Measurements: Technologies and Results, 2009.
- [117] M. V. Trevorrow, S. Vagle, D. M. Farmer. "Acoustical Measurements of Microbubbles within Ship Wakes". The Journal of the Acoustical Society of America, vol. 95, April 1994.
- [118] A. Prosperetti, L. A. Crum, K. W. Commander. "Nonlinear Bubble Dynamics". The Journal of the Acoustical Society of America, vol. 83, February 1988.
- [119] D. R. Jackson, K. B. Briggs. "High-frequency Bottom Scattering: Roughness Versus Sediment Volume Scattering". The Journal of the Acoustical Society of America, vol. 92, August 1992.
- [120] N. Roosnek. "An Acoustic Pipeline Tracking and Survey System for the Offshore". Proceedings of the Eighth European Conference on Underwater Acoustics, ECUA 2006.
- [121] N. Roosnek. "A Torpedo Detection and 3-D Tracking System". Proceedings of the Eighth European Conference on Underwater Acoustics, ECUA 2006.
- [122] J. Kubecka, J. Frouzova, H. Balk, M. Cech, V. Drastik, M. Prchalova. "Regressions for Conversion Between Target Strength and Fish Length in Horizontal Acoustic Surveys". Proceedings of the Third International Conference on Underwater Acoustic Measurements: Technologies and Results, 2009.
- [123] R. Lum, A. Balasuriya, H. Schmidt. "Multistatic Processing and Tracking of Underwater Target Using Autonomous Underwater Vehicles". Proceedings of the Third International Conference on Underwater Acoustic Measurements: Technologies and Results, 2009.
- [124] A. O. Maksimov. "Interpretation of Acoustic Scattering from Submerged Aquatic Vegetation". Proceedings of the Third International Conference on Underwater Acoustic Measurements: Technologies and Results, 2009.

- [125] D. Jeon, F. Pereira, M. Gharib. "Application of DDPIV to Bubbly Flow Measurement". Proceedings of the 11th International Symposium, Application of Laser Techniques to Fluids Mechanics, 2002.
- [126] M. H. Orr, L. R. Haury, P. H. Wiebe, M. G. Briscoe. "Backscatter of High-Frequency (200 kHz) Acoustic Wavefields from Ocean Turbulence". The Journal of the Acoustical Society of America, vol. 108, October 2000.
- [127] M. R. Lewis, B. Johnson, A. Hay. "Backscattering of Spectral Irradiance by Bubbles: HYCODE". Presentation, Satlantic Inc. & Department of Oceanography Dalhousie University.
- [128] Ç. Yardım, Z-H. Michalopoulou, P. Gerstoff. "Bayesian Filters in Ocean Acoustic Applications". Proceedings of the Tenth European Conference on Underwater Acoustics, ECUA 2010.
- [129] K. W. Commander, R. J. McDonald. "Finite-Element Solution of the Inverse Problem in Bubble Swarm Acoustics". The Journal of the Acoustical Society of America, vol. 89, February 1991.
- [130] R. S. Keiffer, J. C. Novarini. "Gauging the Impact that Time Evolving Media and Sea Surfaces Have on the Reverberation Spectrum". Proceedings of the Seventh European Conference on Underwater Acoustics, ECUA 2004.
- [131] T. Ludwicki, P. Cuthbert, S. Spence, T. Kim, J. Mikkelsen, T. McCann. "A Study of Vessel Wakes in Sensitive Inland Waterways". IEEE Conference Proceedings of Oceans 2008.
- [132] J. R. Krieger, G. L. Chahine. "Dynamics and Acoustic Signature of Non-Spherical Underwater Explosion Bubbles". 74th Shock and Vibration Symposium, 2003.
- [133] G. Kapodistrias, P. H. Dahl. "Effects of Interaction Between Two Bubble Scatterers". The Journal of the Acoustical Society of America, vol. 107, 2000.
- [134] A. Poikonen. "High-Frequency Measurements of Underwater Ambient Noise in Shallow Brackish Water". Proceedings of the Tenth European Conference on Underwater Acoustics, ECUA 2010.
- [135] P. A. Elmore, J. W. Caruthers. "Higher Order Corrections to an Iterative Approach for Approximating Bubble Distributions From Attenuation Measurements". IEEE Journal of Oceanic Engineering, vol. 28, no. 1, January 2003.
- [136] T. G. Leighton, P. R. White, D.C. Finfer. "Hypothesis Regarding Exploitation of Bubble Acoustics by Cetaceans". Proceedings of the Ninth European Conference on Underwater Acoustics, ECUA 2008.
- [137] H. Czyz. "Influence of Acoustic Standing Wave on Gas Bubbles in a Liquid - New Results". Proceedings of the Fourth European Conference on Underwater Acoustics, ECUA 1998.

- [138] I. N. Didenkulov, L. M. Kustov, A. I. Martyanov, N. V. Pronchatov-Rubtsov, P. N. Vyugin. "Investigation of the Difference Frequency Scattering from a Cavitation Jet". Proceedings of the Sixth European Conference on Underwater Acoustics, ECUA 2002.
- [139] V. Prokhorov. "Laboratory Modeling of the Sound Scattering by 2D and 3D Stratified Wakes". Proceedings of the Seventh European Conference on Underwater Acoustics, ECUA 2004.
- [140] Z. Klusek. "Linear and Nonlinear Sound Scattering from Subsurface Bubble Layer". Proceedings of the Third European Conference on Underwater Acoustics, ECUA 1996.
- [141] K. W. Commander, A. Prosperetti. "Linear Pressure Waves in Bubbly Liquids: Comparison Between Theory and Experiments". The Journal of the Acoustical Society of America, vol. 85, February 1989.
- [142] T. G. Leighton, A. D. Phelps, M. D. Simpson. "Measurements of the Oceanic Bubble Population Using Propagation Characteristics and Combination Frequency Techniques". Proceedings of the Fourth European Conference on Underwater Acoustics, ECUA 1998.
- [143] H. Czyz, T. Gudra, K. J. Opielinski. "Method of Visualization of Ultrasonic Agglomeration of Gas Bubbles in Liquid". Proceedings of the Sixth European Conference on Underwater Acoustics, ECUA 2002.
- [144] S. Kouzoupis, P. Papadakis. "Modeling of the Swimbladder Sound Producing Mechanism of the European Sea Bass". Proceedings of the Tenth European Conference on Underwater Acoustics, ECUA 2010.
- [145] X. Cristol, J. Dasse, D. Fattaccioli. "Modeling the Low Frequency Acoustic Backscattering from Air Bubble Plumes Associated with Whitecaps". Proceedings of the Tenth European Conference on Underwater Acoustics, ECUA 2010.
- [146] T. Soomere. "Nonlinear Components of Ship Wake Waves". Transactions of the ASME, vol. 60, 2007.
- [147] G. J. Orris, M. Nicholas, M. Querijero. "Non-linear Excitation of Collective Oscillations of Fresh and Salt Water Bubble Plumes". Proceedings of the Second European Conference on Underwater Acoustics, ECUA 1994.
- [148] T. Soomere. "Nonlinear Ship Wake Waves as a Model of Rogue Waves and a Source of Danger to the Coastal Environment: a Review". Oceanologia, vol. 48, 2006.
- [149] I. Yavuz, Z. N. Cehreli, I. B. Celik, S. Shi. "Large Eddy Simulation of the Wake Behind a Turning Ship". Proceedings of the ASME Conference, 2002.
- [150] R. A. Shaw. "Particle-Turbulence Interactions in Atmospheric Clouds". Annual Review of Fluid Mechanics, vol. 35, 2003.

- [151] Z. Ye, H. Hsu, E. Hoskinson. "Phase Order and Energy Localization in Acoustic Propagation in Random Bubbly Liquids". Physics Letters A, Elsevier, October 2000.
- [152] J. M. Fialkowski, R. C. Gauss, D. M. Drumheller. "Predicting near surface scattering statistics using the Poisson-Rayleigh model". Proceedings of the Seventh European Conference on Underwater Acoustics, ECUA 2004.
- [153] A. Sanchez-Caja, J. V. Pylkkanen. "Prediction of Effective Wake at Model and Full Scale Using a RANS Code with an Actuator Disk Model". Second International Conference on Maritime Research and Transportation, 2007.
- [154] R. Sampson. "Presentation of Ship Wakes". Newcastle University, 2010.
- [155] J. A. Nystuen, M. N. Anagnostou, E. N. Anagnostou, A. Papadopoulos. "Real Time Measurements of Physical Conditions at the Sea Surface Using Passive Underwater Acoustics". Proceedings of the Tenth European Conference on Underwater Acoustics, ECUA 2010.
- [156] J. X. Chen, N. V. Lobo, C. E. Hughes, J. M. Moshell. "Real-Time Fluid Simulation in a Dynamic Virtual Environment". Shape and Motion Modeling, 1997.
- [157] I. K. Bjorno, L. Bjorno. "Resonance Properties of Sub-Surface Bubble Clouds". Proceedings of the Second European Conference on Underwater Acoustics, ECUA 1994.
- [158] A. Zak. "Ships Classification Basing On Acoustic Signatures". WSEAS Transactions on Signal Processing, vol. 4, April 2008.
- [159] V. Twersky. "Signals, Scatterers, and Statistics". IEEE Transactions on Antennas and Propagation, November 1963.
- [160] G. L. Chahine. "Software Tool Suite for Bubble Wake Signature of Waterjet Propelled Ships". Dynaflo Inc. Report, 2010.
- [161] D. C. Calvo, M. Zampolli, J. P. Bingham, K. E. Rudd. "Solution of Ocean Acoustic Problems in the Time Domain Using the Elastodynamic Finite Integration Technique". Proceedings of the Tenth European Conference on Underwater Acoustics, ECUA 2010.
- [162] H. A. Burch, S. Vagle, M. J. Buckingham, D. M. Farmer. "Sound Propagation Through the Near-Surface Bubble Layer". Proceedings of the Third European Conference on Underwater Acoustics, ECUA 1996.
- [163] J. K. E. Tunaley. "Status of Ship Wakes in SAR Imagery". London Research and Development Corporation, 2008.
- [164] G. V. Norton, R. D. Purrington, J. C. Novarini. "The Collective Effect of Sea-Surface Roughness, Bottom Roughness and Bubble Plumes on Shallow Water Propagation". Proceedings of the Fifth European Conference on Underwater Acoustics, ECUA 2000.

- [165] J. W. L. Clarke, T. G. Leighton, P. R. White, G. J. Heald, H. A. Dumbrell. "The Effect of Water Quality on the Damping of Bubbles". Proceedings of the Fourth European Conference on Underwater Acoustics, ECUA 1998.
- [166] T. C. Weber, A. P. Lyons, D. L. Bradley. "The Effects of Fluctuating Spatial Structures in Bubble Clouds on the Statistics of Acoustic Propagation". Proceedings of the Seventh European Conference on Underwater Acoustics, ECUA 2004.
- [167] D. M. Farmer, G. B. Deane, S. Vagle. "The Influence of Bubble Clouds on Acoustic Propagation in the Surf Zone". IEEE Journal of Oceanic Engineering, vol. 26, no. 1, January 2001.
- [168] G. V. Norton. "The Numerical Solution of Acoustic Propagation Through Dispersive Moving Media". IEEE Conference Proceedings of OCEANS 2009.
- [169] Z. Klusek. "The Role of Gas Bubbles and Surface-Active Substances on the Noise Generation by Rain Drop". Proceedings of the Sixth European Conference on Underwater Acoustics, ECUA 2002.
- [170] G. Deane, J. Preisig, C. Tindle. "The Scattering of Sound from the Sea Surface: A Deterministic Approach". Proceedings of the Tenth European Conference on Underwater Acoustics, ECUA 2010.
- [171] C. C. Wackerman, W. Pichel, X. Li, C. Jackson. "Toward an Automated Ship and Wake Detection System". Proceedings of OceanSAR, 2006.
- [172] R. A. Shaw, A. B. Kostinski, M. L. Larsen. "Towards Quantifying Droplet Clustering in Clouds". Quarterly Journal of the Royal Meteorological Society, vol. 128, no. 582, 2002.
- [173] S. J. Malinowski, I. Gloza. "Underwater Noise Characteristics of Small Ships". Proceedings of the Sixth European Conference on Underwater Acoustics, ECUA 2002.
- [174] A. Ishimaru. "Wave Propagation and Scattering in Random Media and Rough Surfaces". Proceedings of the IEEE, vol. 79, no. 10, 1991.
- [175] K. Eldhuset. "An Automatic Ship and Ship Wake Detection System for Spaceborne SAR Images in Coastal Regions". IEEE Transactions on Geoscience and Remote Sensing, vol. 34, no. 4, July 1996.
- [176] W. W. Durgin, R. J. Rodenhiser, H. Johari. "Acoustic Technology for Wake Vortex Detection". WakeNet3 - Europe, 2010.
- [177] M. V. Hall. "A Comprehensive Model of Wind-Generated Bubbles in the Ocean and Predictions of the Effects on Sound Propagation at Frequencies up to 40 Khz". The Journal of the Acoustical Society of America, vol. 86, September 1989.
- [178] R. T. Kessel, R. D. Hollett. "Underwater Intruder Detection Sonar for Harbour Protection: State of the Art Review and Implications". NURC Report, 2006.

- [179] A. F. Bunkin, V. K. Klinkov, V. A. Lukyanchenko, S. M. Pershin. "Ship Wake Detection by Raman Lidar". *Applied Optics*, vol. 50, no. 4, February 2011.
- [180] J. A. Kopechek, K. J. Haworth, J. L. Raymond, T. D. Mast, S. R. Perrin, M. E. Klegerman, S. Huang, T. M. Porter, D. D. McPherson, C. K. Holland. "Acoustic Characterization of Echogenic Liposomes: Frequency-Dependent Attenuation and Backscatter". *The Journal of the Acoustical Society of America*, vol. 130, November 2011.
- [181] F. D. Holt, R. L. Culver. "Measuring and Modeling the Bubble Population Produced by an Underwater Explosion". *The Journal of the Acoustical Society of America*, vol. 130, November 2011.
- [182] M. Aydın, A. Şalçı. "Türkiye Sularına Uygun Bir Balıkçı Gemisinin İz Karakteristiklerinin İncelenmesi". *İTÜ Dergisi Mühendislik*, c. 7, Şubat 2008.
- [183] J. Yang, T. K. Sarkar. "Doppler Invariant Property of Hyperbolic Frequency Modulated Waveforms". *Microwave and Optical Technology Letters*, vol. 48, no. 6, June 2006.
- [184] Y. Sun, M. Farooq, LCdr T. K. Robb. "Adaptive CFAR Active Sonar Signal Thresholding Using Radial Basis Functional Neural Networks". *Proceedings of the 36th Conference on Decision & Control*, 1997.
- [185] D. H. Cato, M. J. Noad, D. Stokes, E. Kniest, N. Biassoni, P. Miller, G. B. Deane. "Acoustic and Tracking Techniques in the Humpback Whale Acoustic Collaboration". *Proceedings of the International Conference on Underwater Acoustic Measurements: Technologies & Results*, 2005.
- [186] K. G. Foote, P. R. Atkins, D. T. I. Francis, T. Knutsen. "Measuring Echo Spectra of Marine Organisms over a Wide Bandwidth". *Proceedings of the International Conference on Underwater Acoustic Measurements: Technologies & Results*, 2005.
- [187] I. Starchenko. "Principles of Parametric Array Performance in Moving Water". *Proceedings of the International Conference on Underwater Acoustic Measurements: Technologies & Results*, 2005.
- [188] I. P. Kirsteins, A. Tesei. "Signal Processing Methodologies for Measuring Elastic Wave Backscattering from Symmetric Objects in the Presence of Geometric Interference". *Proceedings of the Second International Conference on Underwater Acoustic Measurements: Technologies and Results*, 2007.
- [189] D. Shuanping, M. Qiming, Z. Lisheng. "Research of Weak Signal Detection Based On Genetic Algorithm". *Proceedings of the Second International Conference on Underwater Acoustic Measurements: Technologies and Results*, 2007.
- [190] R. K. Hansen, U. Castellani, D. Moschini, E. Puppo. "Ping to Ping Registration and Fusion of 3D Sonar Data Sets". *Proceedings of the Second International Conference on Underwater Acoustic Measurements: Technologies and Results*, 2007.

- [191] A. Silva, S. M. Jesus, J. Gomes. "Depth and Range Shift Compensation Using Waveguide Invariant Properties". Proceedings of the Second International Conference on Underwater Acoustic Measurements: Technologies and Results, 2007.
- [192] L. Wang, B. Li, H. Yu, T. TIAN, Q. Li. "The Near-Field Measurement of the Target Radiated Noise by Stolt Interpolation Methods". Proceedings of the Second International Conference on Underwater Acoustic Measurements: Technologies and Results, 2007.
- [193] T. F. Argo, P. S. Wilson. "The Linear Acoustic Behavior of a Bubble Confined Between Parallel Plates". Proceedings of the Second International Conference on Underwater Acoustic Measurements: Technologies and Results, 2007.
- [194] Z. Klusek, J. Jakacki. "The Nonlinear Two-Frequencies Counting of Bubbles Population. Opportunities and Constrains". Proceedings of the Second International Conference on Underwater Acoustic Measurements: Technologies and Results, 2007.
- [195] T. C. Weber, A. P. Lyons, D. L. Bradley. "Identifying Bubble Clustering: Comparisons of the Coherent and Incoherent Fields". Proceedings of the Second International Conference on Underwater Acoustic Measurements: Technologies and Results, 2007.
- [196] D. G. H. Coles, T. G. Leighton. "Autonomous Spar-Buoy Measurements of Bubble Populations under Breaking Waves in the Sea of the Hebrides". Proceedings of the Second International Conference on Underwater Acoustic Measurements: Technologies and Results, 2007.
- [197] T. G. Leighton, J. W. L. Clarke, G. J. Heald, H. A. Dumbrell, R. C. Evans. "Application of the Nonlinear Acoustic Scatter Cross-Section to the Use of Clinical Ultrasound Contrast Agents". ISVR Technical Memorandum, University of Southampton, February 1999.
- [198] S. Pashazadeh, M. Sharifi. "Determining the Best Sensing Coverage for 2-Dimensional Acoustic Target Tracking". Sensors, May 2009.
- [199] A. Prosperetti, Y. Hao. "Modelling of Spherical Gas Bubble Oscillations and Sonoluminescence". Phil. Trans. R. Soc. Lond. A, vol. 357, 1999.
- [200] L. Solomon. "Multi-Purpose Acoustic Target Tracking for Additive Situational Awareness". Army Research Laboratory Report, November 2008.
- [201] A. H. Nayfeh, D. T. Mook. "Nonlinear Response of a Spherical Bubble to a Multi-Frequency Excitation". Journal de Physique, November 1979.
- [202] T. Kawamura, A. Fujiwara, . "The Effects of the Bubble Size on the Bubble Dispersion and Skin Friction Reduction". Proceedings of the 5th Symposium on Smart Control of Turbulence, 2004.
- [203] X. Di, K. E. Gilbert. "Wave Propagation in a 3-D Turbulent Atmosphere: Horizontal Coherence". The Proceedings of the 8th International Symposium on Long-Range Sound Propagation, September 1998.

- [204] X. Di, K. E. Gilbert. "Wave Propagation in a 3-D Turbulent Atmosphere: Horizontal Coherence". The Proceedings of the 8th International Symposium on Long-Range Sound Propagation, September 1998.
- [205] W. R. Blanding, P. K. Willett, Y. Bar-Shalom, R. S. Lynch. "Directed Subspace Search ML-PDA with Application to Active Sonar Tracking". IEEE Transactions on Aerospace and Electronic Systems, January 2008.
- [206] N. Kumar, Q. F. Tan, S. S. Narayanan. "Object Classification in Sidescan Sonar Images with Sparse Representation Techniques". Proceedings of the International Conference on Acoustics, Speech and Signal Processing, March 2012.
- [207] R. Pinkel, M. Merrifield, J. Smith, H. Ramm. "Advances in Doppler Sonar Technology". Proceedings of the IEEE Fifth Working Conference on Current Measurement, 1995.
- [208] A. Mantouka, T. G. Leighton, A. I. Best, J. K. Dix, P. R. White. "Inferring Bubble Populations in Intertidal Sediments From Attenuation and Scattering Measurements". Proceedings of the Third International Conference on Underwater Acoustic Measurements: Technologies and Results, 2009.
- [209] A. O. Maksimov. "Characteristics of Acoustic Scattering from Hydrate Shelled Bubbles". Proceedings of the Third International Conference on Underwater Acoustic Measurements: Technologies and Results, 2009.
- [210] A. Sutin, B. Bunin. "Acoustic Research for Port Protection at the Stevens Maritime Security Laboratory". Proceedings of the Third International Conference on Underwater Acoustic Measurements: Technologies and Results, 2009.
- [211] R. S. Khan. "A Simple Model of Ship Wakes". M.S. Thesis, The University of British Columbia, September 1994.
- [212] P. Elisseff. "Modelling of Underwater Ambient Noise Due to Whitecaps". M.S. Thesis, Florida Atlantic University, April 1992.
- [213] A. A. Ruffa. "A Finite Element Analysis of Acoustic Wave Propagation Through Bubbly Liquids". Ph.D. Thesis, Yale University, December 1990.
- [214] D. Kurennoy. "Analysis of the Properties of Fast Ferry Wakes in the Context of Coastal Management". Ph.D. Thesis, Tallinn University of Technology, 2009.
- [215] W. P. Arnott. "Generalized Glory Scattering from Spherical and Spheroidal Bubble in Water: Unfolding Axial Caustics with Harmonic Angular Perturbations of Toroidal Wavefronts". Ph.D. Thesis, Washington State University, August 1988.
- [216] S. L. Ceccio. "Observations of the Dynamics and Acoustics of Travelling Bubble Cavitation". Ph.D. Thesis, California Institute of Technology, August 1990.
- [217] P. S. Wilson. "Sound Propagation and Scattering in Bubbly Liquids". Ph.D. Thesis, Boston University, 2002.
- [218] J. D. Muench. "Periodic Acoustic Radiation from a Low Aspect Ratio Propeller". Ph.D. Thesis, University of Rhode Island, 2001.

[219] K. Hsiao, H. de Plinval-Salgues, J. Miller. "Particle Filters and Their Applications". Cognitive Robotics, 2005.

[220] F. Gustafsson, F. Gunnarsson, N. Bergman, U. Forssell, J. Jansson, R. Karlsson, P. J. Nordlund. "Particle Filters for Positioning, Navigation and Tracking". IEEE Transactions on Signal Processing, vol. 50, no. 2, February 2002.

[221] L. Svensson. "Comments on the Resampling Step in Particle Filtering"., March 2012.

[222] M. S. Arulampalam, S. Maskell, N. Gordon, T. Clapp. "A Tutorial on Particle Filters for Online Nonlinear/Non-Gaussian Bayesian Tracking". IEEE Transactions on Signal Processing, vol. 50, no. 2, February 2002.

[223] Ç. Önür, K. Leblebicioğlu. "Ship Wake Acoustic Tracking Using Particle Filter". IEEE Journal of Oceanic Engineering, 2013.

[224] Ç. Önür, K. Leblebicioğlu. "Wake Tracking with Particle Filter". 21. IEEE Sinyal İşleme ve İletişim Uygulamaları Kurultayı, 2013.

CURRICULUM VITAE

PERSONAL INFORMATION

Surname, Name: Önür, Çağla
Nationality: Turkish (TC)
Date and Place of Birth: 14 October 1977, Ankara
Marital Status: Single
Phone: +90 533 474 81 52
e-mail: caglaonur@yahoo.com

EDUCATION

Degree	Institution	Year of Graduation
MS	METU Electrical and Electronics Engineering	2001
BS	METU Electrical and Electronics Engineering	1998
High School	T.E.D Ankara College, Ankara	1994

WORK EXPERIENCE

Year	Place	Enrollment
2008-	STM Savunma Teknolojileri Mühendislik ve Tic. A.Ş.	Senior Systems Engineer, Consultant
2006-2007	TÜBİTAK-SAGE	Expert Researcher
2004-2005	Başkent University, Department of Electrical and Electronics Eng.	Research Assistant
1998-2004	METU, Department of Electrical and Electronics Engineering	Research Assistant

FOREIGN LANGUAGES

English